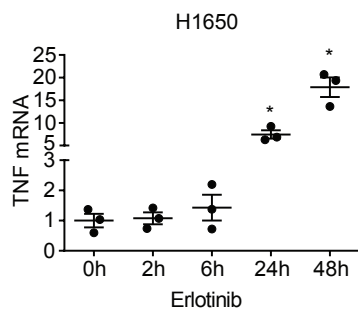
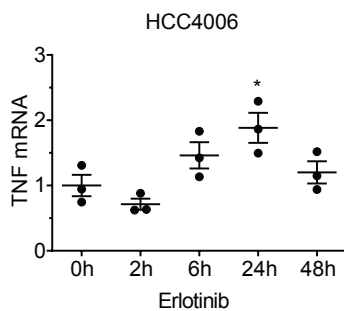


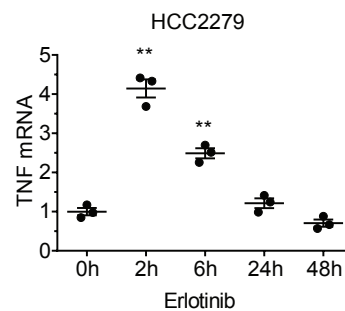
A



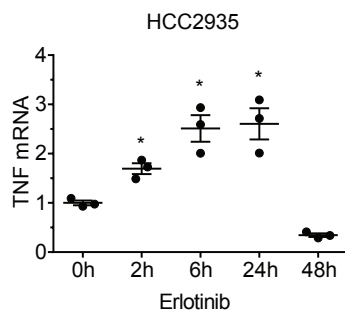
B



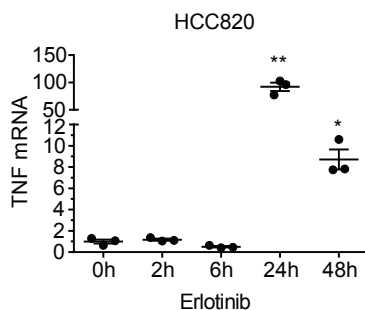
C



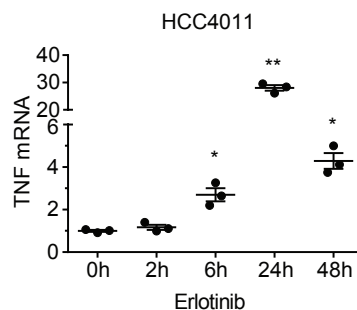
D



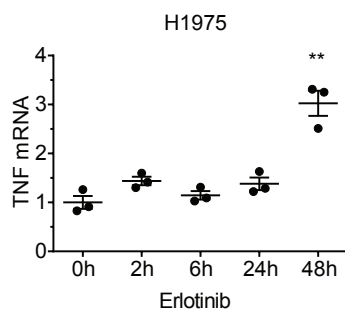
E



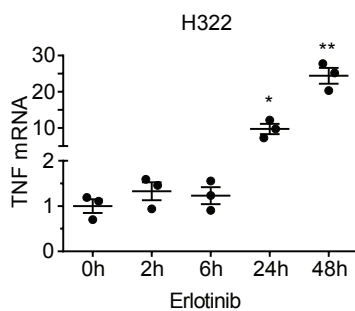
F



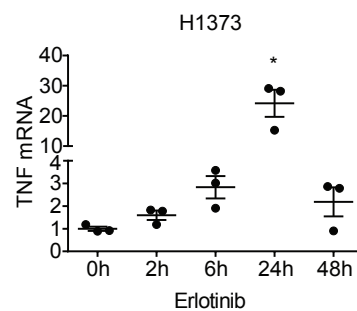
G



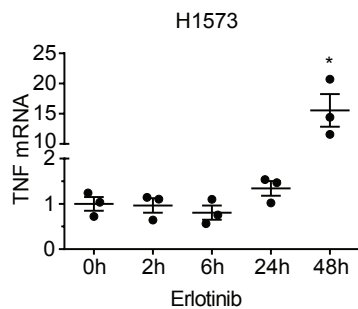
H



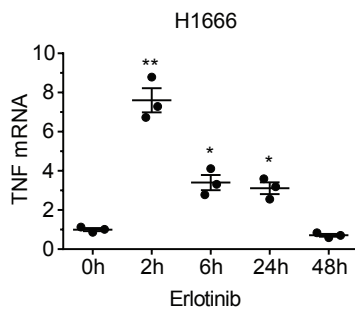
I



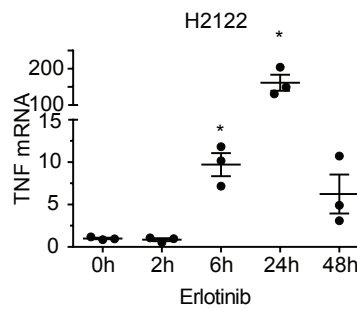
J



K



L



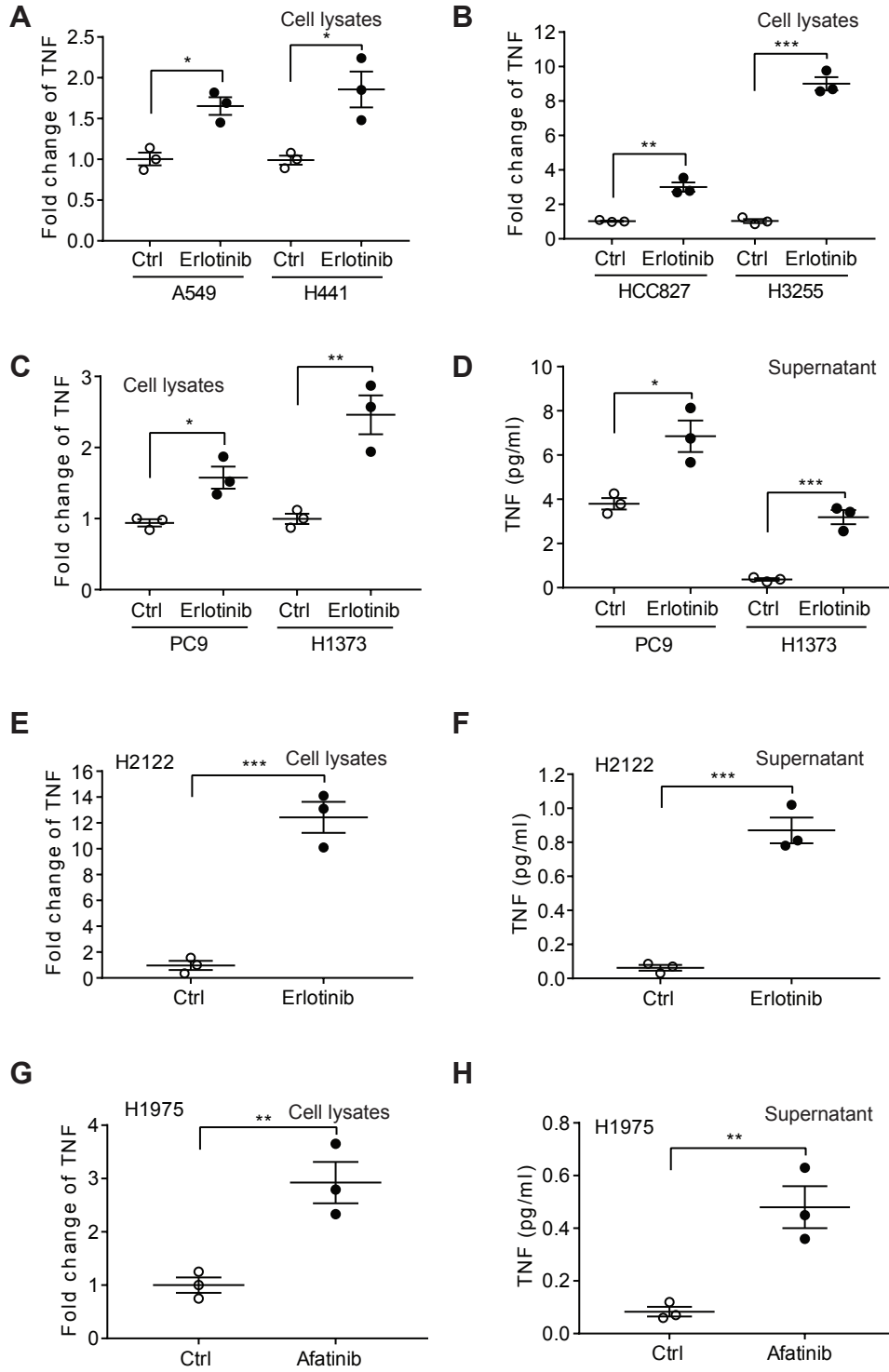
Supplementary Figure Legends:

Supplementary Figure 1: EGFR inhibition induced upregulation of TNF mRNA

A-L NSCLC cell lines were cultured in RPMI-1640 in 5% FBS and were treated with erlotinib (100nM for EGFR mutant cell lines and 1 μ M for EGFR wild type cell lines) for the times indicated followed by RNA extraction and quantitative real time PCR for TNF. Data represent the mean \pm SEM. n=3 biologically independent experimental replicates. * P <0.05 and ** P <0.01, by Student's t test.

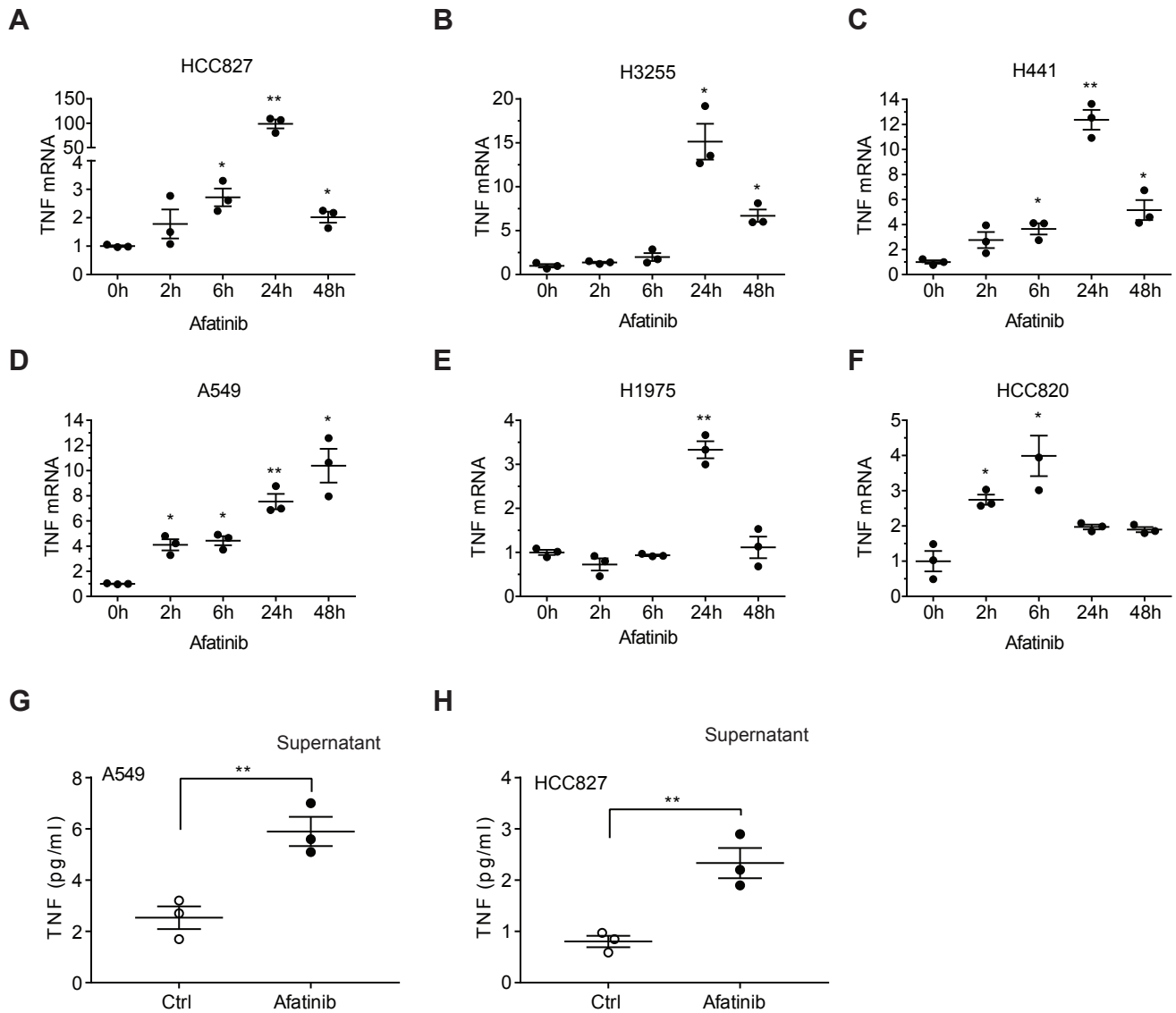
Supplementary Figure 2

Gong, Guo et al.



Supplementary Figure 2: EGF inhibition induces TNF upregulation at a protein level

A-C. NSCLC cells were cultured in serum free medium and exposed to erlotinib for 48 hours followed by preparation of cell lysates and level of TNF protein was measured by ELISA. D. PC9 or H1373 cells were treated with erlotinib and the TNF level was measured in the supernatant by ELISA. E-F. H2122 cells were exposed to erlotinib for 48 hours, followed by preparation of cell lysates and supernatant, TNF level in cell lysates and supernatant was measured by ELISA. G. H1975 cells were exposed to afatinib (100nM) for 48 hours followed by preparation of cell lysates and supernatant, TNF level in cell lysates or supernatant was measured by ELISA. The erlotinib concentration used was 100nM for EGFR mutant cell lines and 1 μ M for EGFR wild type cell lines. Data represent the mean \pm SEM. n=3 biologically independent experimental replicates. * P < 0.05, ** P < 0.01 and *** P < 0.001, by Student's t test.

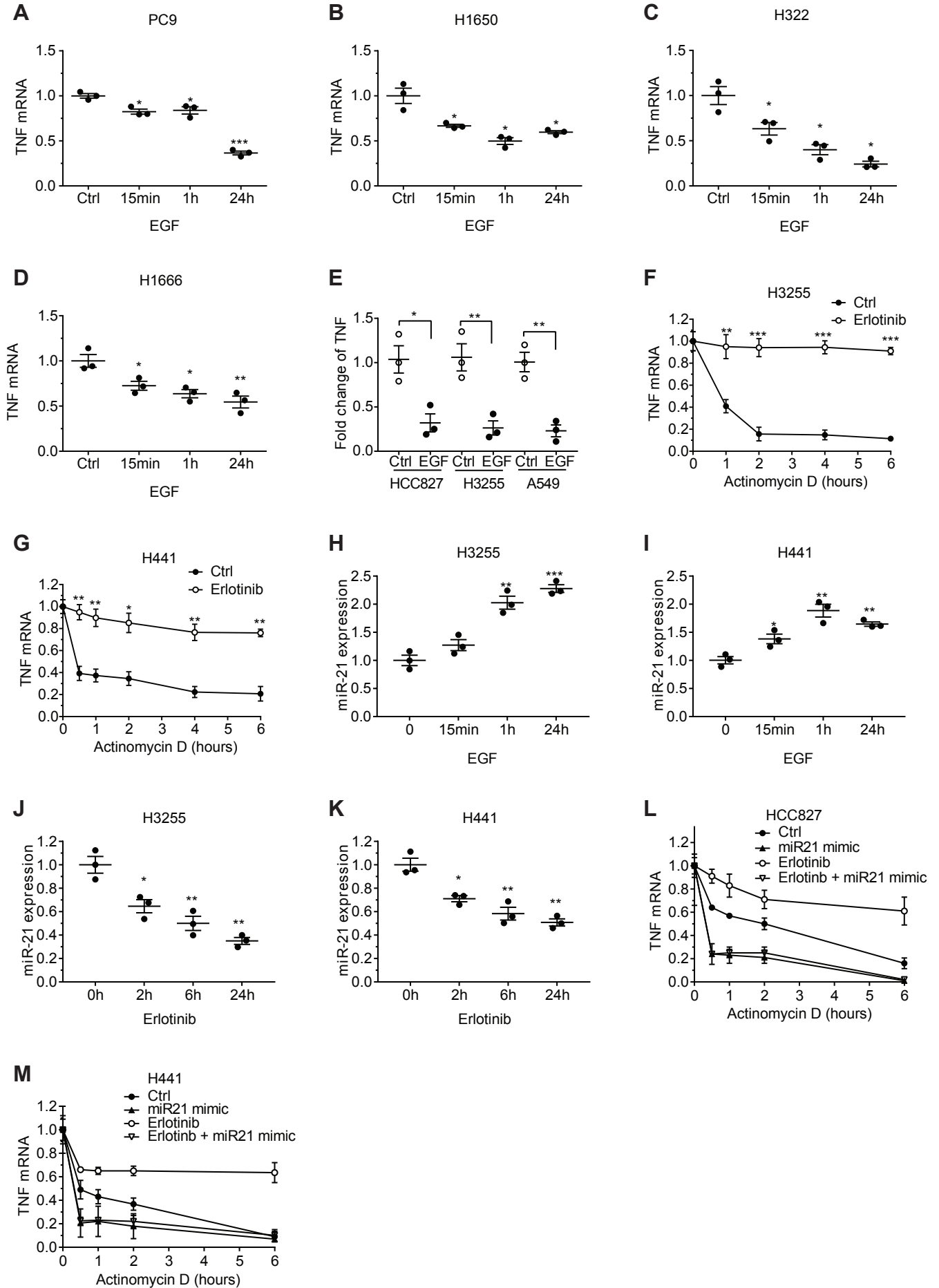


Supplementary Figure 3: Afatinib induces upregulation of TNF in lung cancer cell lines

A-F: NSCLC cell lines were cultured in RPMI-1640 in 5% FBS and were treated with afatinib (100nM) for the times indicated followed by RNA extraction and quantitative real time PCR for TNF. G-H: A549 or HCC827 cells were treated with afatinib (1 μ M or 100nM) and the TNF level was measured in the supernatant by ELISA. Data represent the mean \pm SEM. n=3 biologically independent experimental replicates. * P <0.05, ** P <0.01 and *** P <0.001, by Student's t test.

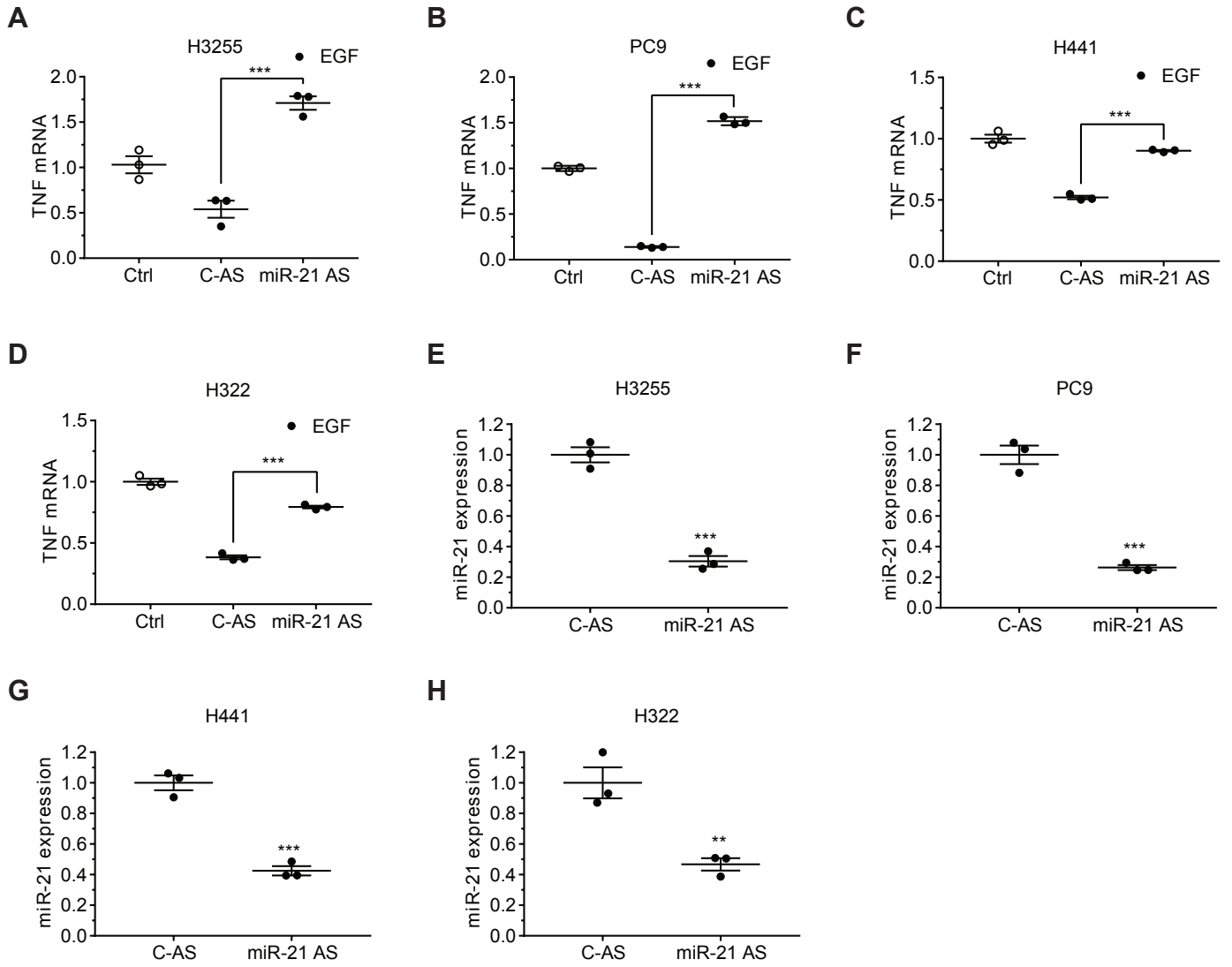
Supplementary Figure 4

Gong, Guo et al.



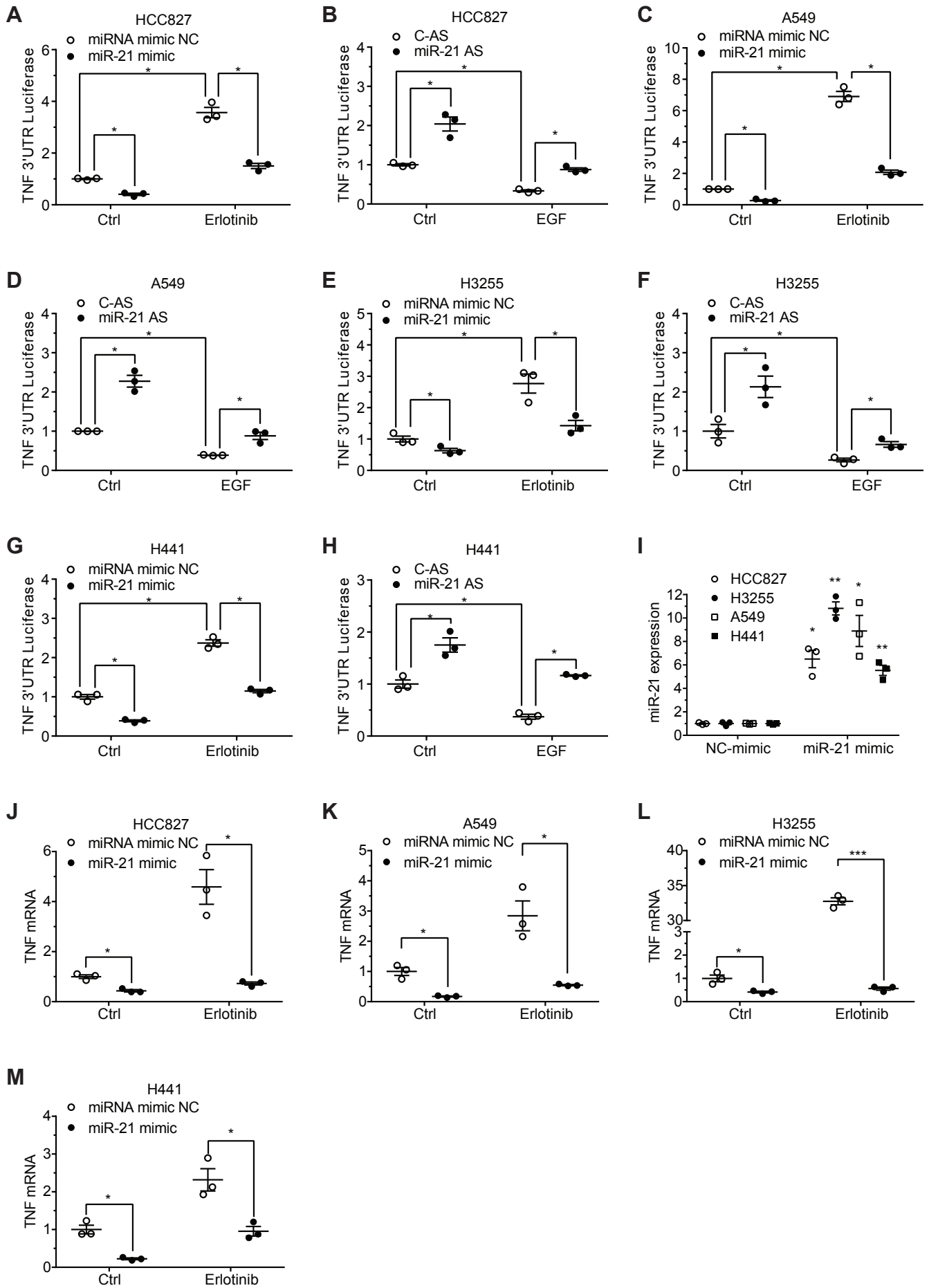
Supplementary Figure 4: EGFR activity regulates miR-21

A-D NSCLC cell lines were exposed to EGF (50ng/mL) for the indicated time points followed by qRT-PCR for TNF mRNA. E. Regulation of TNF level in multiple cell lines by EGF treatment detected by ELISA. F. H3255 Cells were treated with Actinomycin D (5µg/mL) and erlotinib (100nM) for the indicated time points followed by RNA extraction and qRT-PCR for TNF mRNA. G. A similar experiment was done in H441 cells using an erlotinib concentration of 1µM. H-I miR-21 expression was examined in H3255 and H441 cells following exposure to EGF for the indicated time points followed by qRT-PCR using a TaqMan Human MicroRNA Assay kit. J-K H3255 or H441 cells were exposed to Erlotinib (100nM or 1µM) for the indicated time points followed by qRT-PCR for miR-21 using a TaqMan Human MicroRNA Assay kit. L-M. Cells were treated with Actinomycin D (5µg/mL) and erlotinib (100nM) in the presence or absence of miR-21 ,mimic for the indicated time points followed by RNA extraction and qRT-PCR for TNF mRNA. Data represent the mean ± SEM. n=3 biologically independent experimental replicates. * $P < 0.05$, ** $P < 0.01$ and *** $P < 0.001$, by Student's t test.



Supplementary Figure 5: EGFR activity regulates TNF mRNA stability mediated by upregulation of miR-21

A-D H3255, PC9, H441 or H322 cells were transfected with a control antisense oligonucleotide (C-AS) or a miR-21 antisense oligonucleotide (miR-21 AS) for 48h followed by exposure of cells to EGF for 1h and qRT-PCR for TNF. In E-H, the downregulation of miR-21 by the miR-21 antisense oligonucleotide was confirmed. In all experiments involving the use of EGF, cells were serum starved overnight. Data represent the mean \pm SEM. n=3 biologically independent experimental replicates. * P <0.05, ** P <0.01 and *** P <0.001, by Student's t test.

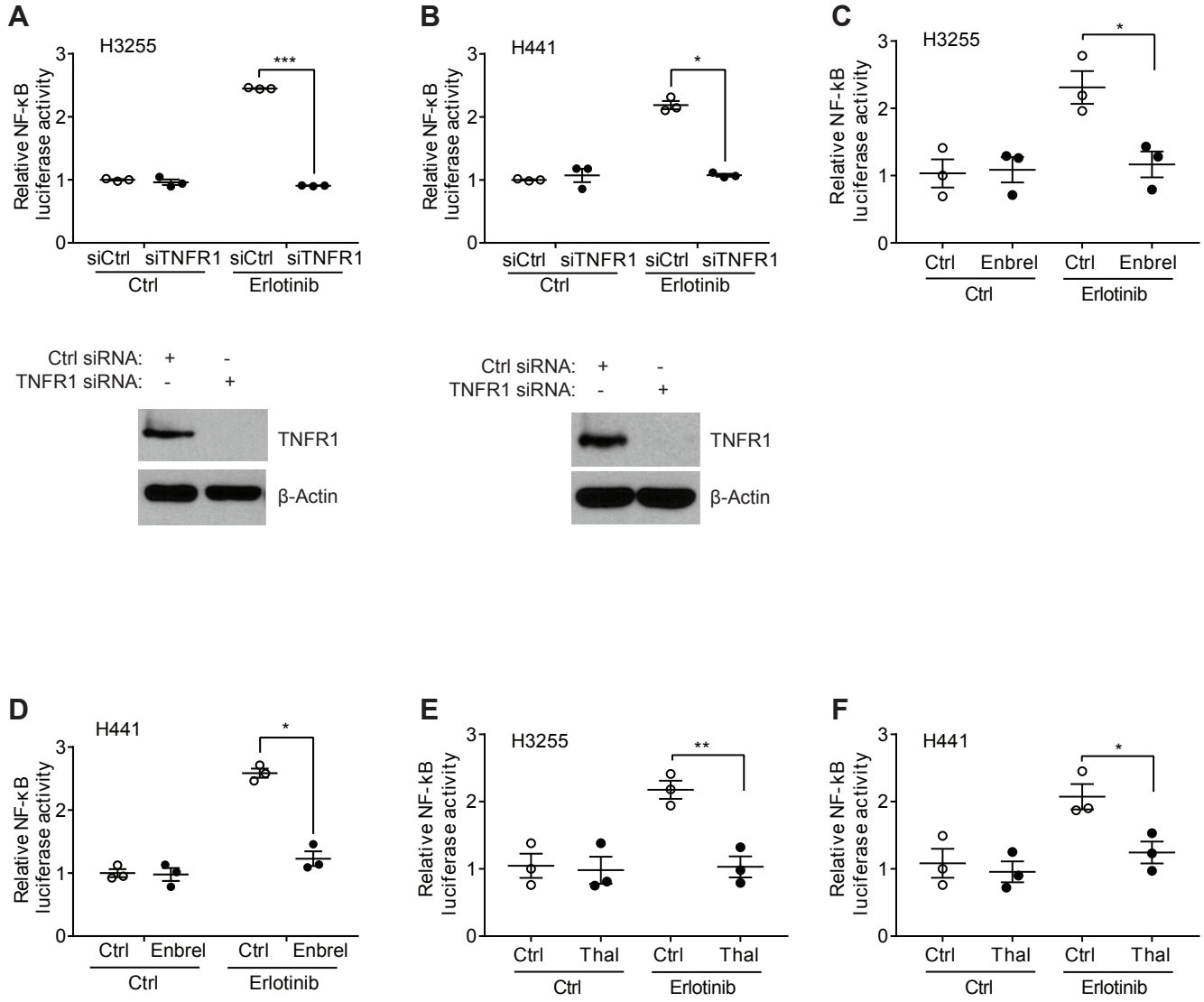


Supplementary Figure 6: EGFR regulates TNF expression via miR-21.

A. HCC827 cells were co-transfected with TNF 3'UTR luciferase reporter (SV40-luc-TNF) and miR-21 mimic or miRNA mimic negative control for 48 hours, then cells were exposed to erlotinib for additional 24 hours. TNF 3'UTR luciferase activities were detected by a luciferase assay. B. HCC827 cells were co-transfected with TNF 3'UTR luciferase reporter (SV40-luc-TNF) and miR-21 AS for 48 hours, followed by incubation with EGF. TNF 3'UTR luciferase activities were detected by a luciferase assay. C-H. Similar experiments were performed on A549, H3255, and H441 cells. I. Overexpression of miR-21 mimic was confirmed by qPCR. J-M. NSCLC cells were transfected with miR-21 mimic or control mimic for 48 hours. After that, cells were exposed to erlotinib for 24 hours, followed by qRT-PCR for detecting TNF mRNA levels. The dose of erlotinib used was 100 nM for EGFR mutant cells and 1 μ M for EGFRwt cells. In all experiments involving the use of EGF, cells were serum starved overnight. Data represent the mean \pm SEM. n=3 biologically independent experimental replicates. * P < 0.05, ** P < 0.01, by Student's t test.

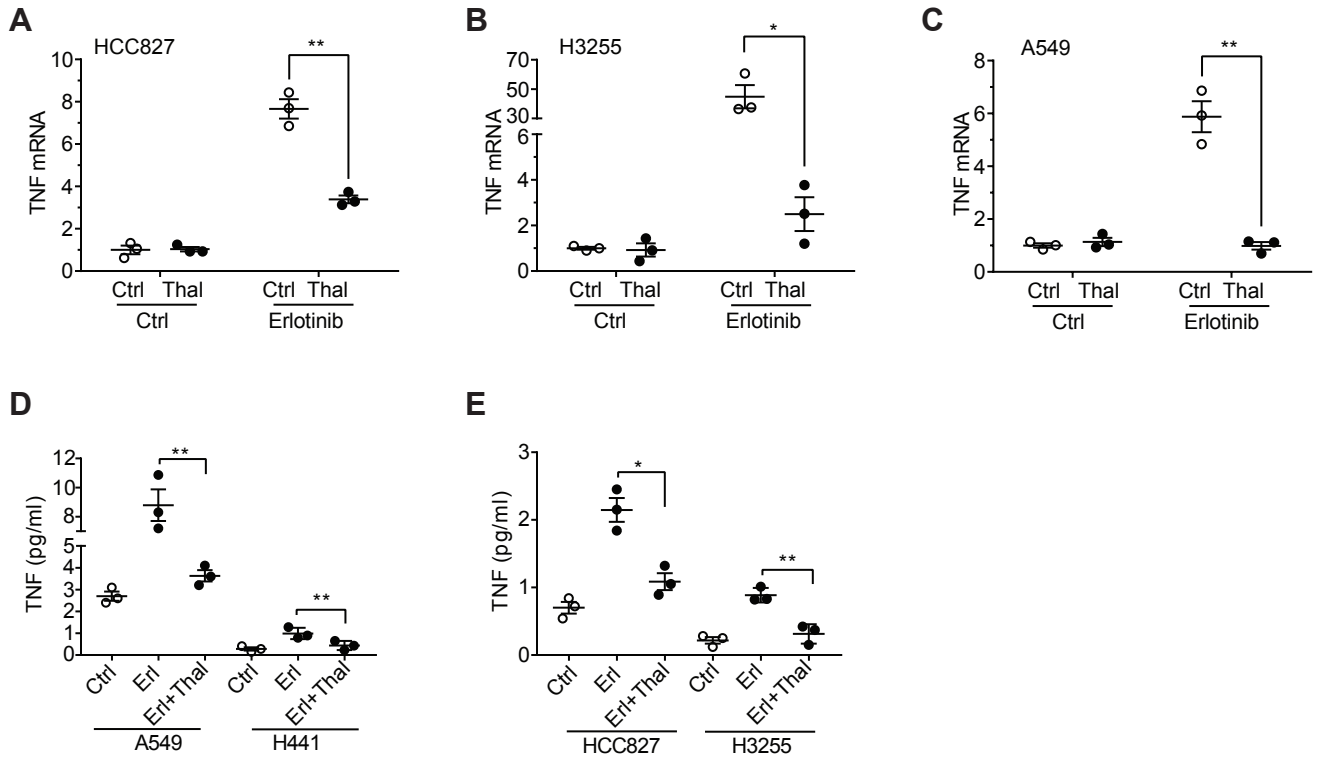
Supplementary Figure 7

Gong, Guo et al.



Supplementary Figure 7: EGFR inhibition induces a TNF-dependent activation of NF- κ B

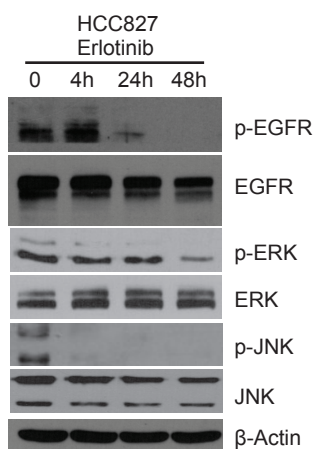
A-B. siRNA knockdown of TNFR1 was performed in H3255 or H441 cells followed by transfection of cells with an NF- κ B luciferase reporter and exposure of cells to erlotinib following by a reporter assay. Silencing of TNFR1 was confirmed with a Western blot. Western blots are representative of at least three independent replicates. C. A TNF blocking drug Etanercept (Enbrel) was used at a concentration of 100 μ g/mL along with erlotinib for 24h followed by a reporter assay in H3255 cells. D. A similar experiment was conducted in H441 cells. E-F. Reporter assay for NF- κ B in H3255 or H441 cells treated with erlotinib in the presence or absence of thalidomide (5 μ g/mL). Data represent the mean \pm SEM. n=3 biologically independent experimental replicates. * P < 0.05, ** P < 0.01 and *** P < 0.001, by Student's t test.



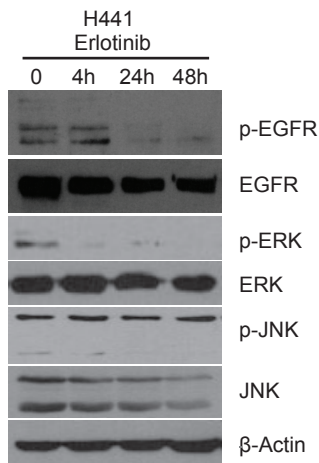
Supplementary Figure 8 Thalidomide blocks upregulation of TNF in response to EGFR inhibition.

A-C. Cells were pretreated with thalidomide (5 µg/mL) for 1 hour, followed by addition of erlotinib. (HCC827 and H3255 100nM, A549 1 µM). 24 hours later mRNA was isolated from untreated or treated cells. TNF mRNA was measured by qRT-PCR. Erlotinib induced TNF mRNA levels was significantly decreased by thalidomide. D-E. Cells were cultured in serum free medium and pretreated with thalidomide (5µg/mL) for 1 hour, followed by addition of erlotinib (HCC827, H3255 100nM; H441, A549 1µM). After 48 hours supernatant was collected and concentrated. The levels of TNF protein in supernatant were measured by ELISA. Erlotinib increases levels of TNF protein, which was significantly reduced by thalidomide. Data represent the mean ± SEM. n=3 biologically independent experimental replicates. * $P < 0.05$ and ** $P < 0.01$ by Student's t test.

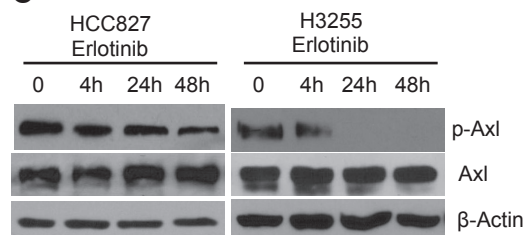
A



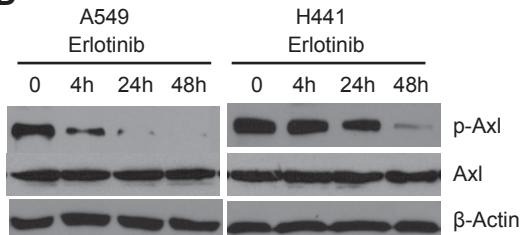
B



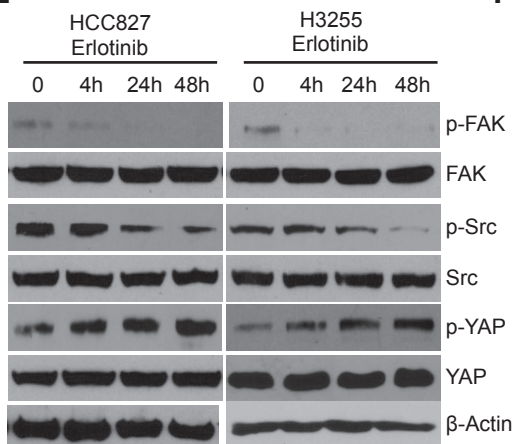
C



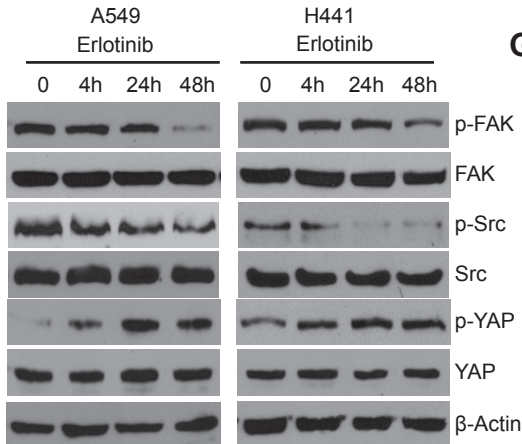
D



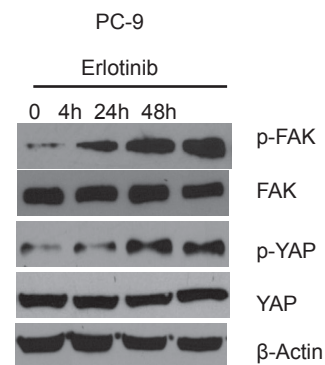
E



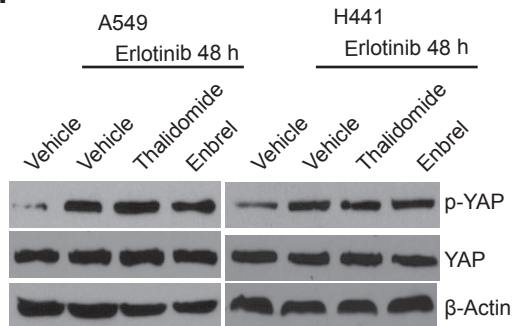
F



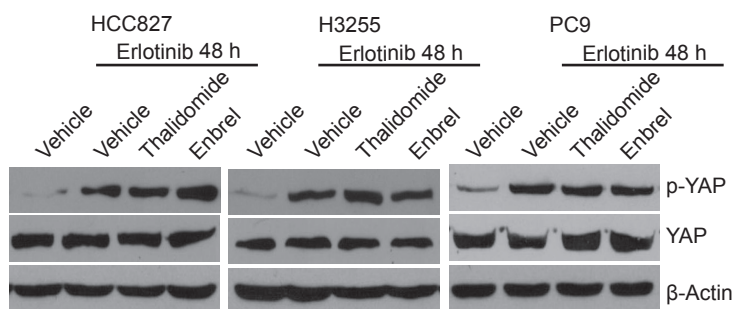
G



H



I

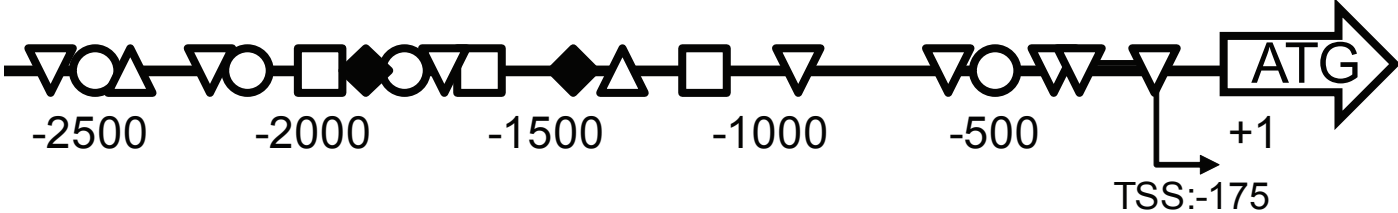


Supplementary Figure 9: The effect of Erlotinib on additional signaling pathways

A-D. EGFR inhibition with erlotinib is unable to reactivate pJNK, ERK or pAxl in lung cancer cell lines. A-B. HCC827 and H441 cells were treated with 100nM and 1 μ M erlotinib respectively. Protein samples were collected at indicated time point. pEGFR, pERK and pJNK were detected by western blot. C. HCC827 and H3255 cells were treated with erlotinib (100nM) for the indicated time points followed by western blot with the pAxl antibody. D. Similar experiments were conducted in A549 and H441 cells except that erlotinib concentration is 1 μ M. E-F. Erlotinib downregulates both Src and Fak activation but activates YAP in lung cancer cells. E. HCC827 and H3255 cells were exposed to erlotinib (100nM) for the indicated time points followed by western blot with the indicated antibodies. F. Similar experiments were performed in A549 and H441 cells except that erlotinib concentration is 1 μ M. G. PC-9 cells were treated with 100nM erlotinib for the indicated time points followed by western blot with the indicated antibodies. H-I. Erlotinib induced pYAP in lung cancer cells could not be blocked by thalidomide or enbrel. Cells were treated with erlotinib in the presence or absence of thalidomide (5 μ g/mL) or enbrel (100 μ g/mL) for 48 hours, followed by western blot with an anti-pYAP antibody. Erlotinib concentration is consistent with the experiments described in E-G. Western blots shown are representative of at least three independent experiments.

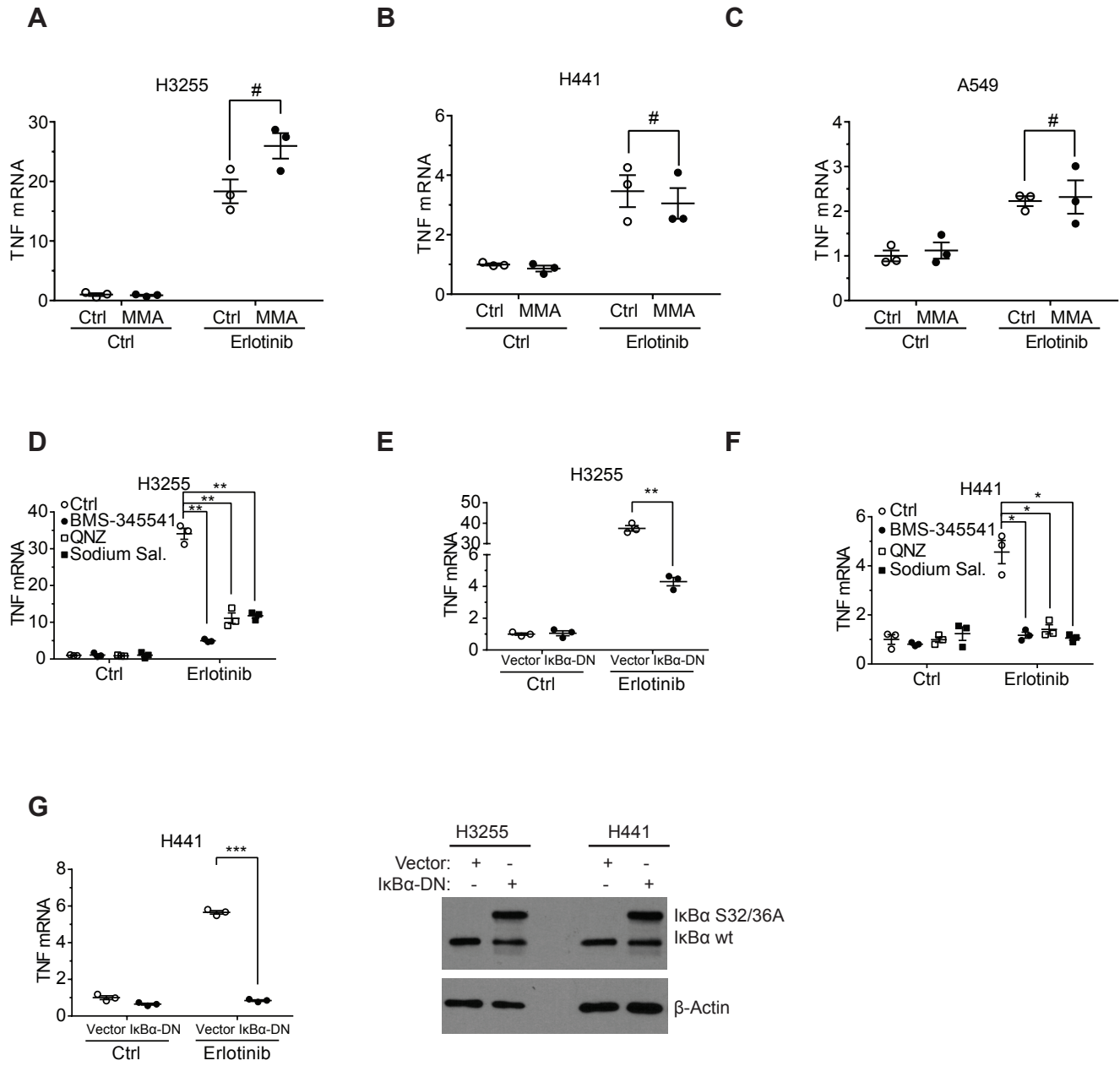
Human TNF gene promoter

□ C/EBP ○ AP1 ◆ NF-κB △ GATA-1 ▽ SP1



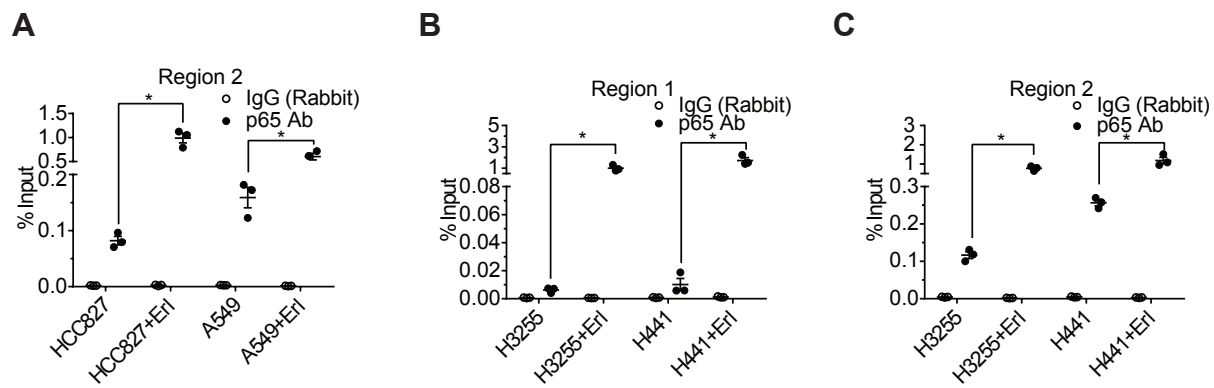
Supplementary Figure 10: Transcriptional sites in the TNF promoter.

A schematic of the TNF promoter showing sites for major transcription factors.



Supplementary Figure 11: Sp1 inhibition fails to inhibit erlotinib-induced upregulation of TNF mRNA.

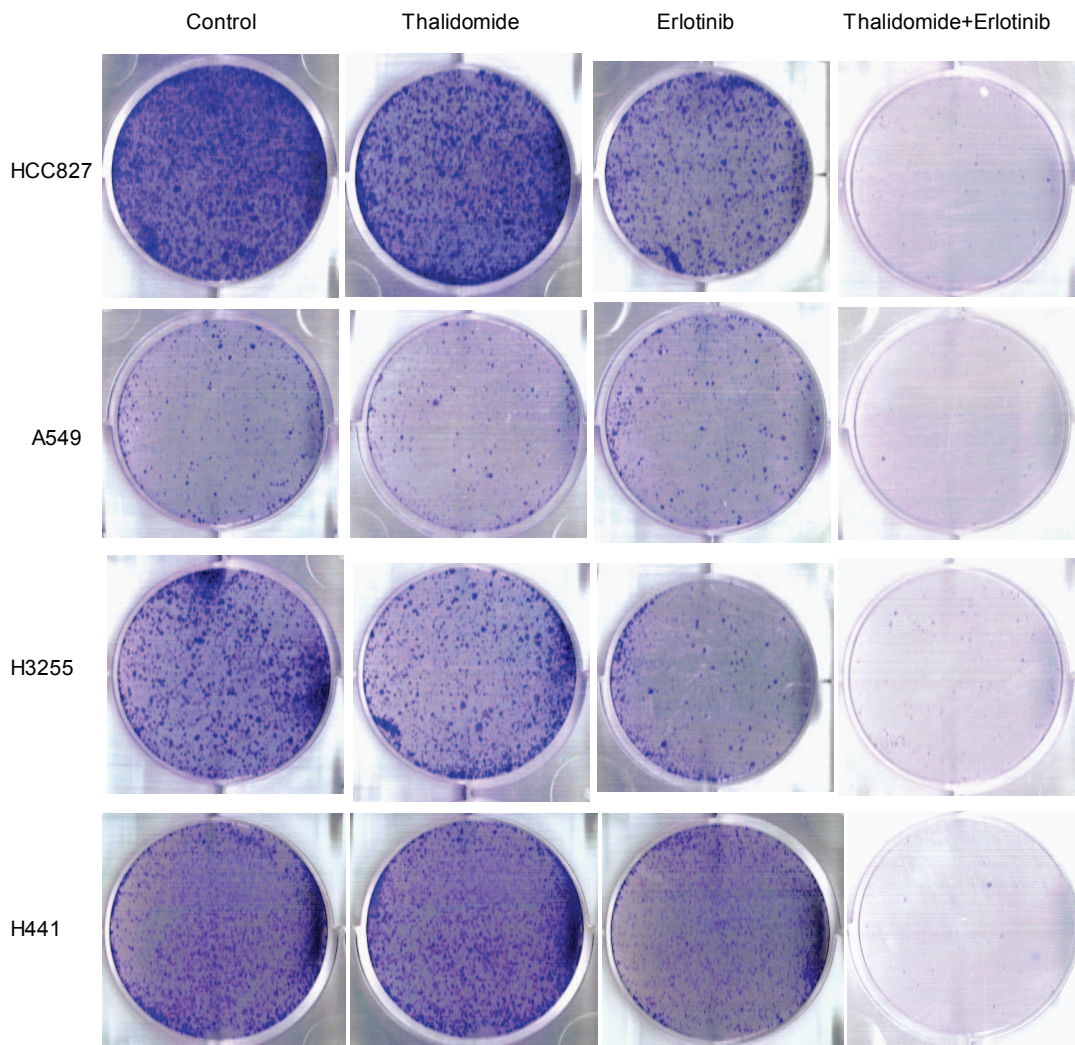
A-C: Inhibition of Sp1, using Mithramycin (1 μ M), fails to inhibit erlotinib-induced TNF upregulation in various cell lines. Cells were pretreated with Mithramycin for 1h followed by erlotinib addition for 24h, followed by qRT-PCR for TNF mRNA. D. 1 hour pretreatment of NF- κ B inhibitors (100 nM BMS-345541, 1 μ M QNZ, and 5 mM Sodium Salicylate) inhibited erlotinib-upregulated TNF in H3255 cells, as determined by qRT-PCR. E. I κ B α -DN over-expression blocks erlotinib-induced upregulation of TNF in H3255 cells. F-G. The same experiment as D-E conducted in H441 cells. I κ B α -DN over-expression was confirmed by Western blot. The mutant protein migrates slower on electrophoretic gels. The dose of erlotinib used is 100 nM in H3255 cell, and 1 μ M in A549 and H441 cells, all for 24 hours. Data represent the mean \pm SEM. n=3 biologically independent experimental replicates. *P<0.05, **P<0.01, ***P<0.001, # indicates not statistically significant, by Student's t test when comparing two indicated groups, or One-way ANOVA, Dunnett's method for comparing multiple groups to the same control (D and F). Western blots shown are representative of at least three independent experiments.



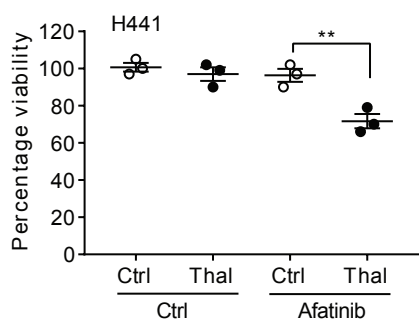
Supplementary Figure 12: Increased NF- κ B at the TNF gene promoter in response to EGFR inhibition

A-C CHIP-qPCR shows a minor NF- κ B p65 antibody enrichment (percentage of input, comparing to rabbit IgG) over putative NF- κ B binding region 2 on TNF promoter in HCC827 and A549 cells, as well as both region 1 and 2 in H3255 and H441 cells, which can be further enhanced significantly after 1 μ M (H441) or 100 nM (H3255) Erlotinib treatment for 24 hours. Data represent the mean \pm SEM. n=3 biologically independent experimental replicates. * P < 0.05 by Student's t test.

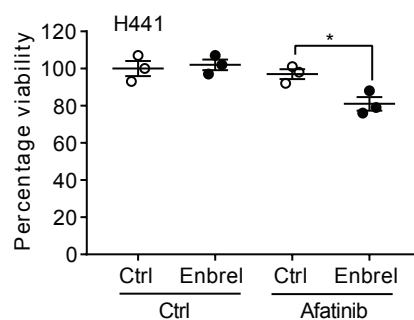
A



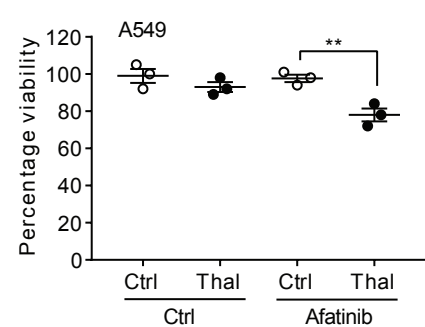
B



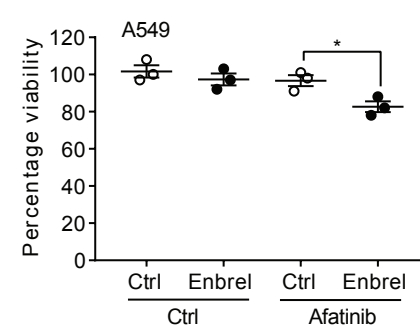
C



D



E



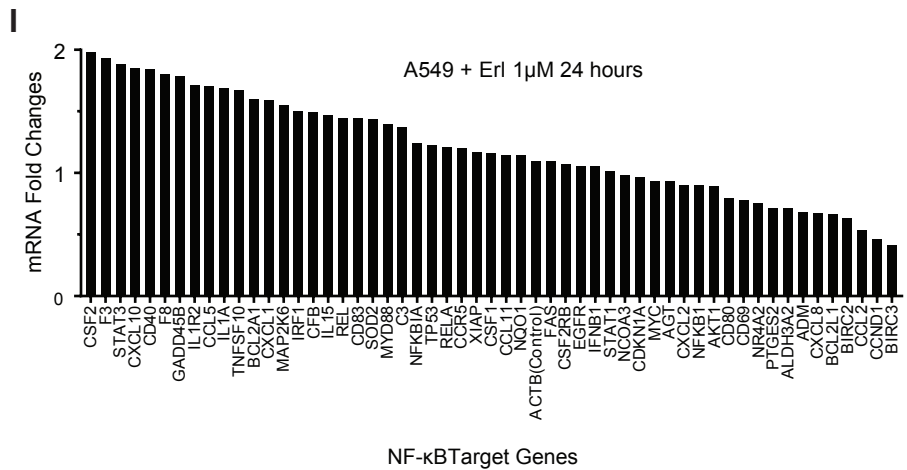
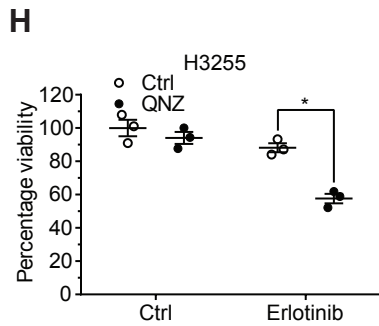
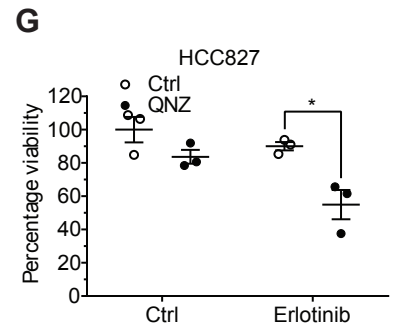
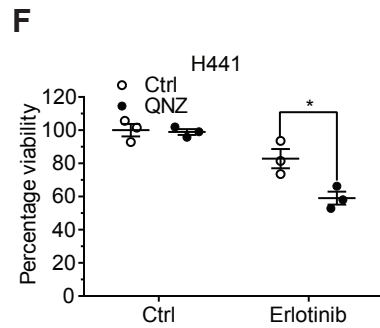
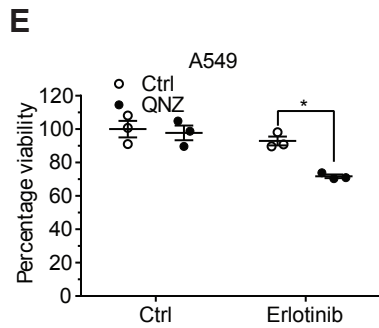
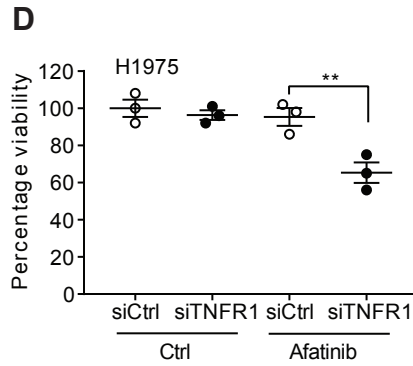
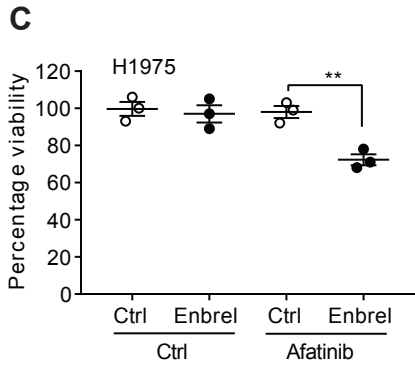
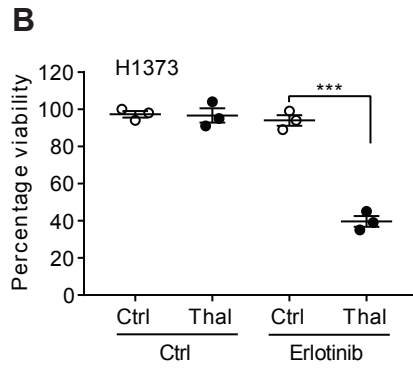
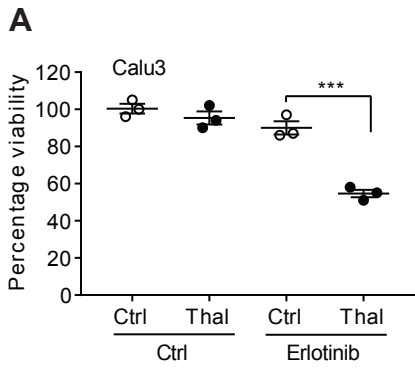
100nM Afininib

Supplementary Figure 13: TNF inhibition sensitizes lung cancer cell lines to EGFR inhibition

A. EGFR wt and mutant NSCLC cells were seeded in 6 well plates at 1000 cells/well, and incubated under 5 µg/mL Thalidomide and/or Erlotinib of 10 nM (for EGFR mutant cells HCC827 and H3255) or 1µM (for EGFRwt A549 cells). 14 days later, cell colonies were fixed by 100% methanol and then stained by 0.5% crystal violet in 25% methanol. Images were captured by a scanner and colony counting was processed by ImageJ. Images shown are representative of at least three independent replicates. B. Thalidomide (5µg/mL) and afatinib were added concurrently and AlamarBlue assay was done after 72h. C. A similar experiment was done using Enbrel (100µg/mL) and afatinib in H441 cells. D. A similar AlamarBlue assay was conducted in A549 cells with afatinib and thalidomide. E. A similar AlamarBlue assay was conducted in A549 cells with afatinib and Enbrel. The afatinib concentration in these experiments was 100nM. For B-E, data represent the mean ± SEM. n=3 biologically independent experimental replicates. * $P < 0.05$, ** $P < 0.01$ and *** $P < 0.001$, by Student's t test.

Supplementary Figure 14

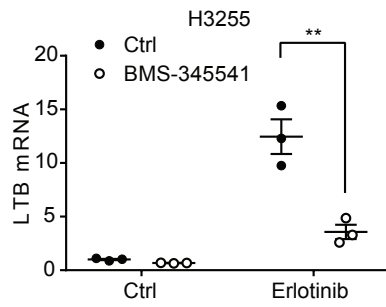
Gong, Guo et al.



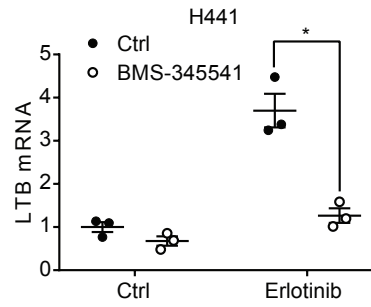
Supplementary Figure 14: Biological effects of a combined EGFR and TNF/NF- κ B inhibition in additional lung cancer cell lines and EGFR inhibition's effects on additional NF- κ B target genes

A-B Calu-3 and H1373 cells were cultured in RPMI-1640 with 5% FBS and treated with erlotinib (1 μ M) or thalidomide (5 μ g/mL) or a combination for 72h followed by an AlamarBlue assay. C. H1975 cells were cultured in RPMI-1640 with 5% FBS and treated with afatinib (100nM) or thalidomide (5 μ g) or a combination for 72h followed by an AlamarBlue assay. D. H1975 cells were cultured in RPMI-1640 with 5% FBS and treated with afatinib (100nM) or Enbrel (100 μ g/mL) or a combination for 72h followed by an AlamarBlue assay. D. AlamarBlue assay in H1975 cells. TNFR1 was silenced using siRNA and cells were exposed to afatinib for 72h in RPMI-1640 with 5% FBS. Silencing of TNFR1 was confirmed by Western blot by at least three independent experiments. E-H. NSCLC cell lines were exposed to erlotinib with or without NF- κ B inhibitor QNZ: 6-amino-4-(4-phenoxyphenylethylamino) quinazoline (1 μ M) for 72h followed by an AlamarBlue assay. I. EGFR inhibition promotes expression of NF- κ B target genes. Cells were treated with 1 μ M Erlotinib or DMSO for 24 hours. The extracted RNA was subjected to Human NF- κ B Signaling Targets PCR Array. The panel displays genes with fold changes less than 2. Western blots are representative of at least three independent experiments. For A-H, data represent the mean \pm SEM. n=3 biologically independent experimental replicates. * P < 0.05, ** P < 0.01 and *** P < 0.001, by Student's t test.

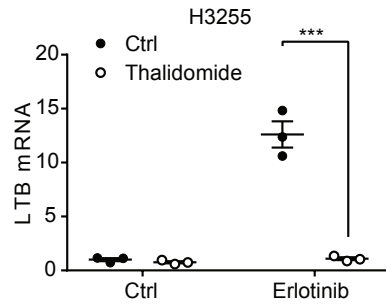
A



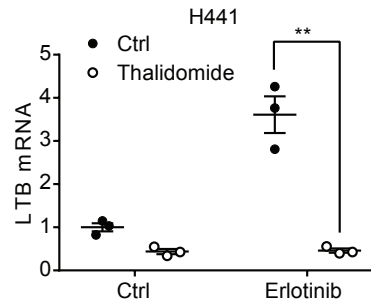
B



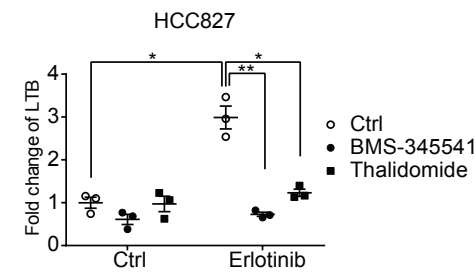
C



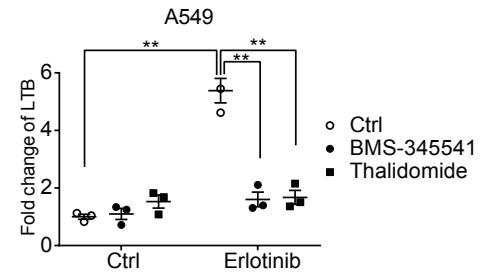
D



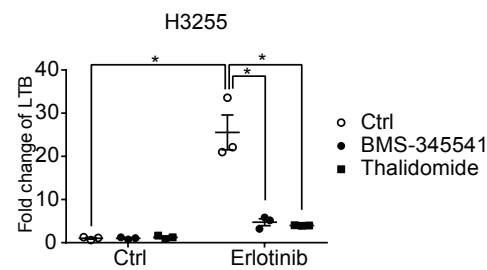
E



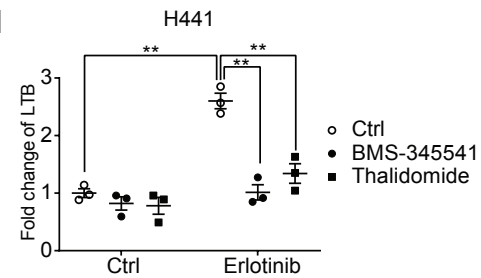
F



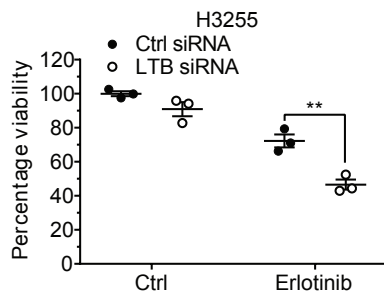
G



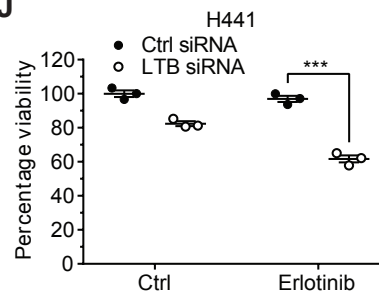
H



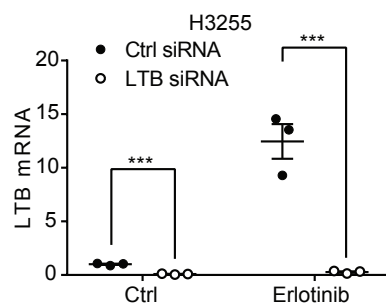
I



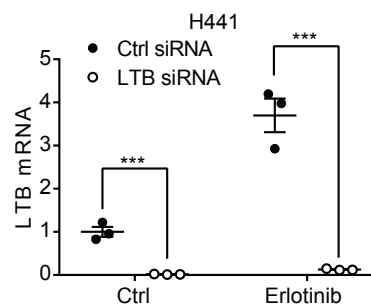
J



K



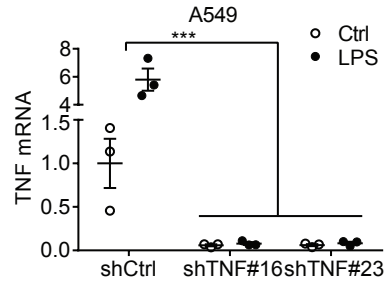
L



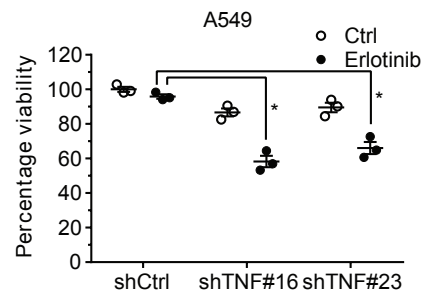
Supplementary Figure 15: Inhibition of LT β sensitizes EGFRwt and EGFR mutant NSCLC to EGFR inhibition

A-D. H3255 and H441 cells were pretreated with 100nM BMS-345541 or 5 μ g/mL thalidomide for 1 hour, and then exposed to erlotinib for 24 hours. LT β mRNA was detected by qPCR. E-H. NSCLC cells were treated with erlotinib, in the presence or absence of 100nM BMS-345541 or thalidomide 5 μ g/mL for 24 hours. LT β expression levels were tested by Homo TNFC (LT β) Colorimetric Cell-Based ELISA Kit. I-J. H3255 and H441 cells were transfected with LT β siRNA or control siRNA for 48 hours, then erlotinib was added for additional 72 hours. An Alamar Blue assay was performed to investigate cell viabilities. K-L. LT β qPCR was used to confirm the silence effects of siRNA. Data represents the mean \pm SEM. n=3 biologically independent experimental replicates. * P < 0.05, ** P < 0.01, and *** P < 0.001, by Student's t test.

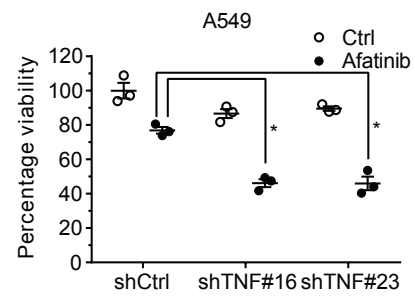
A



B

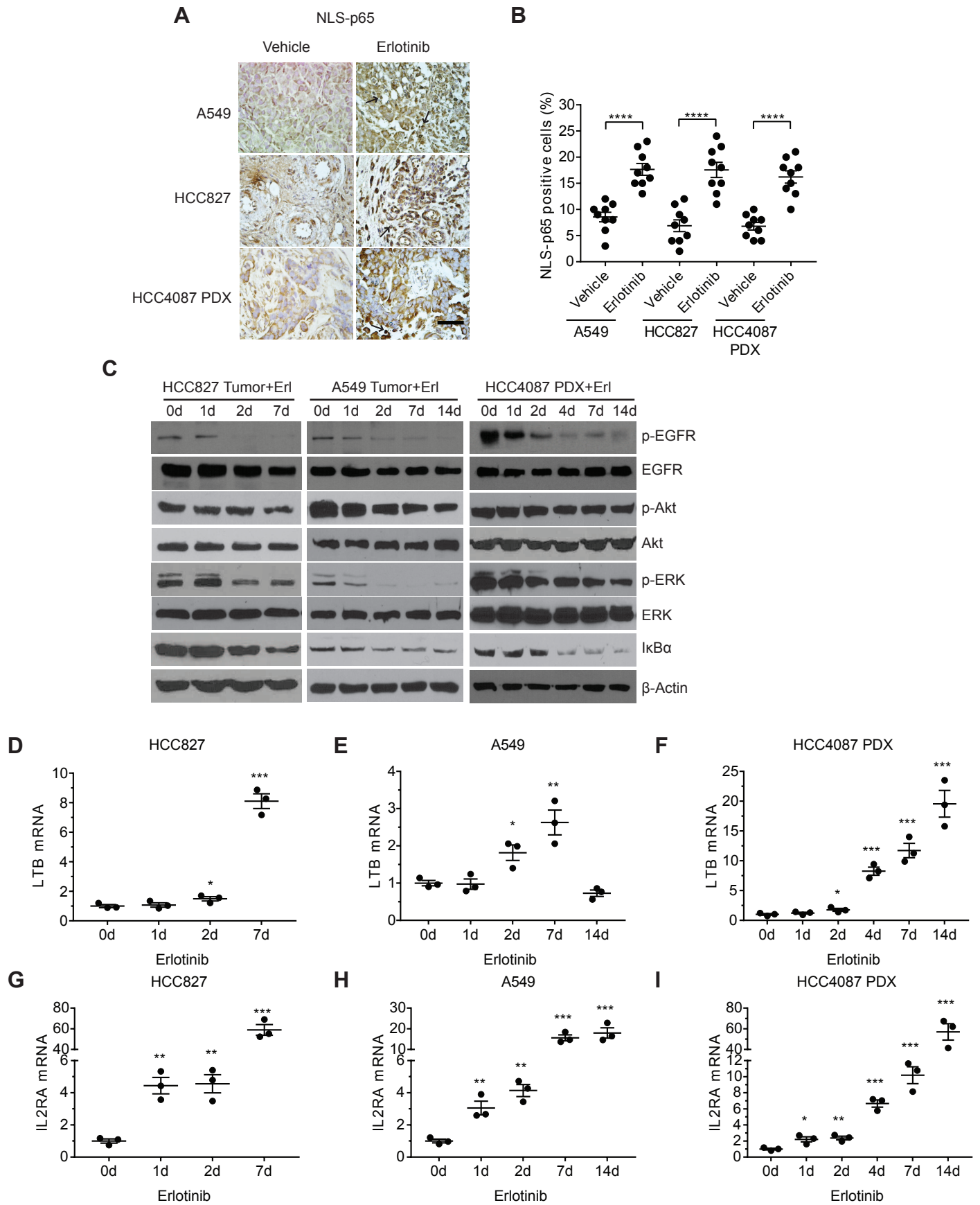


C



Supplementary Figure 16: Biological and signaling consequences of TNF silencing in A549 cells:

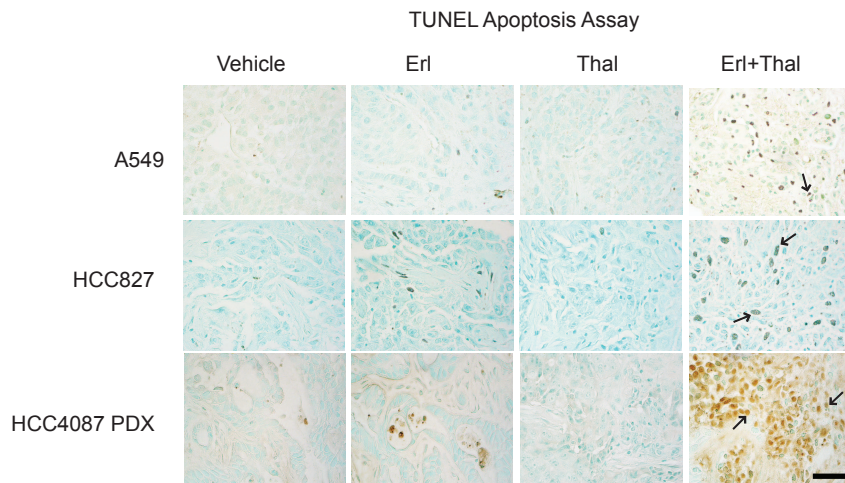
A. Stable silencing of TNF in A549 cells was done with isolation of two clones with low basal and LPS induced TNF (#16 and #23) as determined by qRT-PCR. B-C. A549 cells with stable silencing of TNF (clones 16 and 23) or control shRNA were exposed to erlotinib or afatinib (1 μ M) for 72h followed by an AlamarBlue cell viability assay. Data represent the mean \pm SEM. n=3 biologically independent experimental replicates (A-E). * P < 0.05 and *** P < 0.001, by Student's t test.



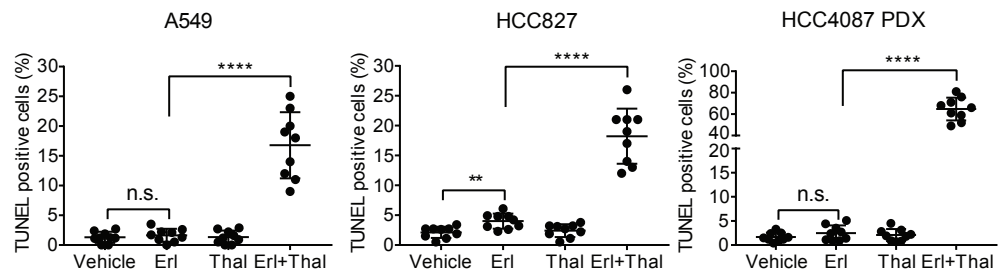
Supplementary Figure 17: Erlotinib induces activation of NF- κ B and upregulation of NF- κ B regulated downstream genes *in vivo*

A. Immunostaining of nuclear localized p65 from a representative subcutaneous tumor section from mice bearing subcutaneous tumors treated with vehicle or erlotinib for 7 days as described in Figure 1 (n=3 mice per group). Nuclear localization of NF- κ B subunit p65 is indicated by black arrows. Scale bar: 50 μ m. B. Quantification of p65 positive cells. Three fields (x400) were randomly selected for each tissue block (n=9). C. Signal transduction in xenograft tumors exposed to erlotinib. Tumor lysates were collected for the indicated time points followed by Western blot with the indicated antibodies. D-I. The mRNA levels of NF- κ B target genes, LT β and IL2RA were detected in subcutaneous tumors from mice treated with erlotinib as discussed above (n=3 mice per group). Data represent the mean \pm SEM. * P <0.05, ** P < 0.01, *** P <0.001, and **** P <0.0001, by Student's t test. Western blots shown are representative of three independent experiments.

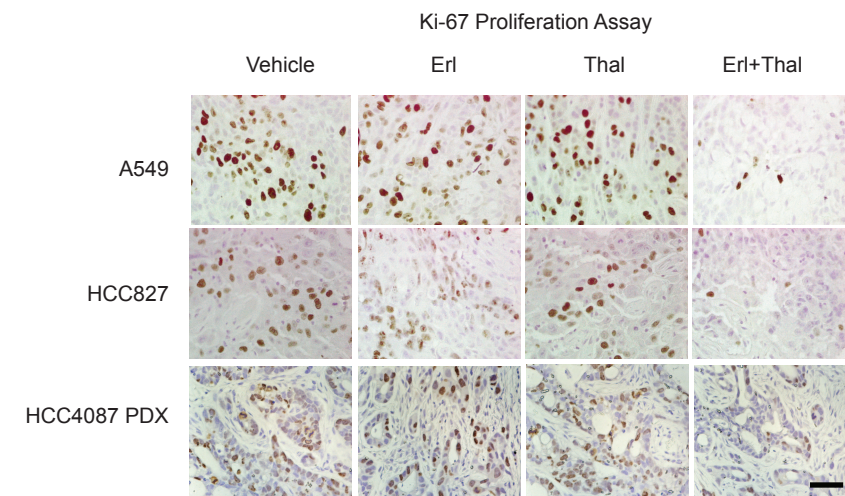
A



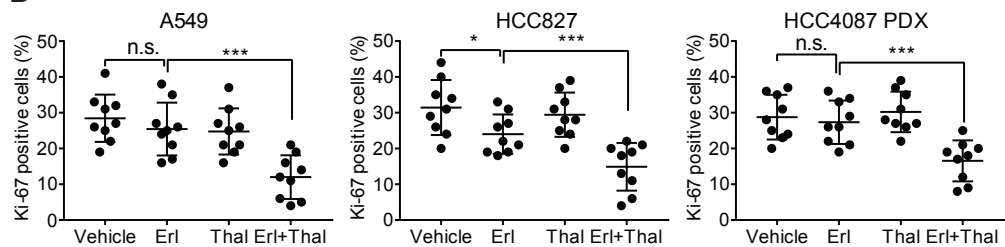
B



C



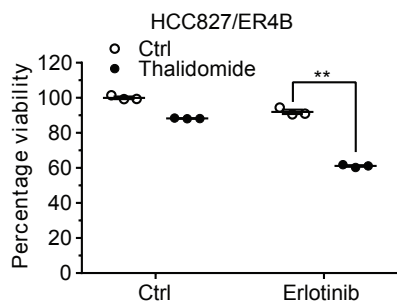
D



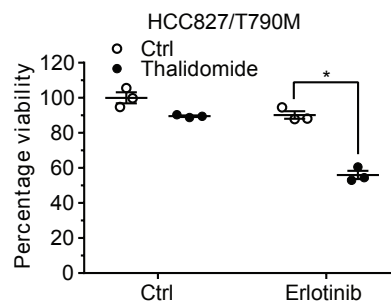
Supplementary Figure 18: Erlotinib plus thalidomide treatment inhibits proliferation and induces apoptosis in human lung cancer xenograft tumors

A. Apoptotic cell death was measured by TUNEL assay in FFPE tissue sections from subcutaneous tumors. TUNEL positive cells are indicated by black arrows. Representative images of subcutaneous tumors from vehicle, erlotinib (Erl), thalidomide (Thal) and erlotinib plus thalidomide group as described in figure 8 (n=3 mice per group). Scale bar: 50 μ m. B. Quantification of TUNEL positive tumor cells. Three fields (x400) were randomly selected for each tissue block (n=9). C. Proliferation was measured by Ki-67 staining. Representative images of subcutaneous tumors from vehicle, erlotinib (Erl), thalidomide and erlotinib plus thalidomide group as described in figure 8 (n=3 mice per group). Scale bar: 50 μ m. D. Quantification of Ki-67 positive tumor cells. Three fields (x400) were randomly selected for each tissue block (n=9). Data represent the mean \pm SEM. * P < 0.05, ** P < 0.01, *** P < 0.001, and **** P < 0.0001, by Student's t test.

A



B

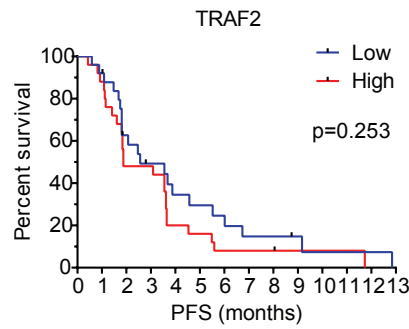
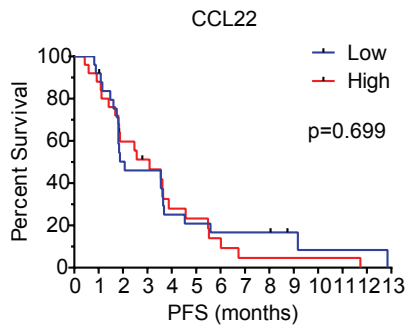
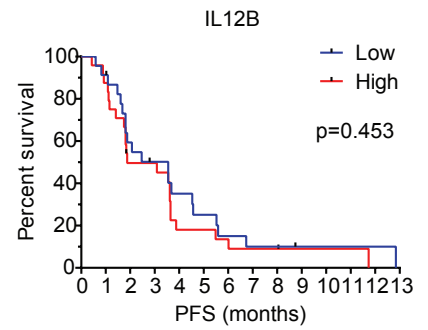
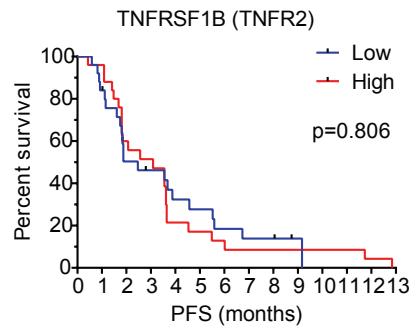
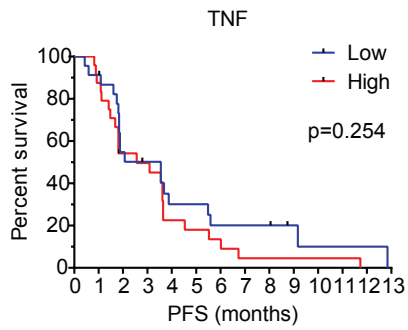
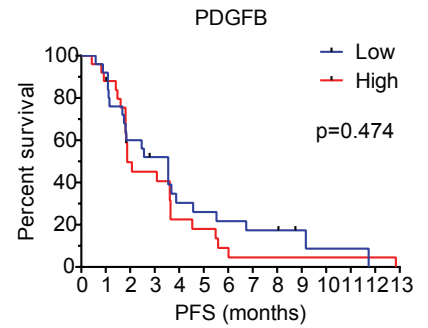
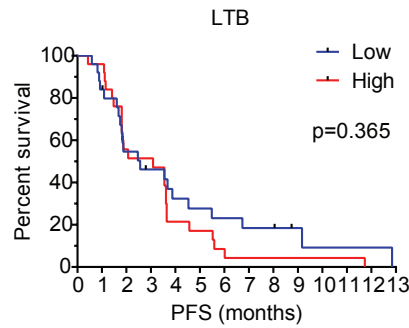
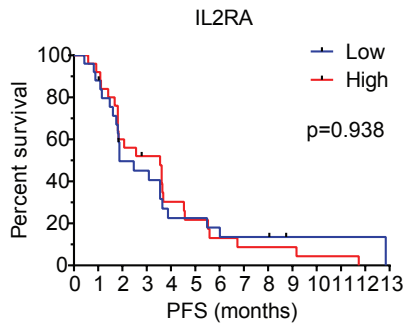


Supplementary Figure 19 Combination of EGFR and TNF inhibition on additional EGFR mutant and erlotinib resistant cell lines

A-B. HCC827/ER4B and HCC827/T790M cells were treated with 5µg/mL thalidomide and/or 100nM erlotinib for 72 hours and analyzed by AlamarBlue assay. Data represents mean ± SEM. n=3 biologically independent experimental replicates. *P <0.05, **P <0.01, by Student's t test.

Supplementary Figure 20

Gong, Guo et al.

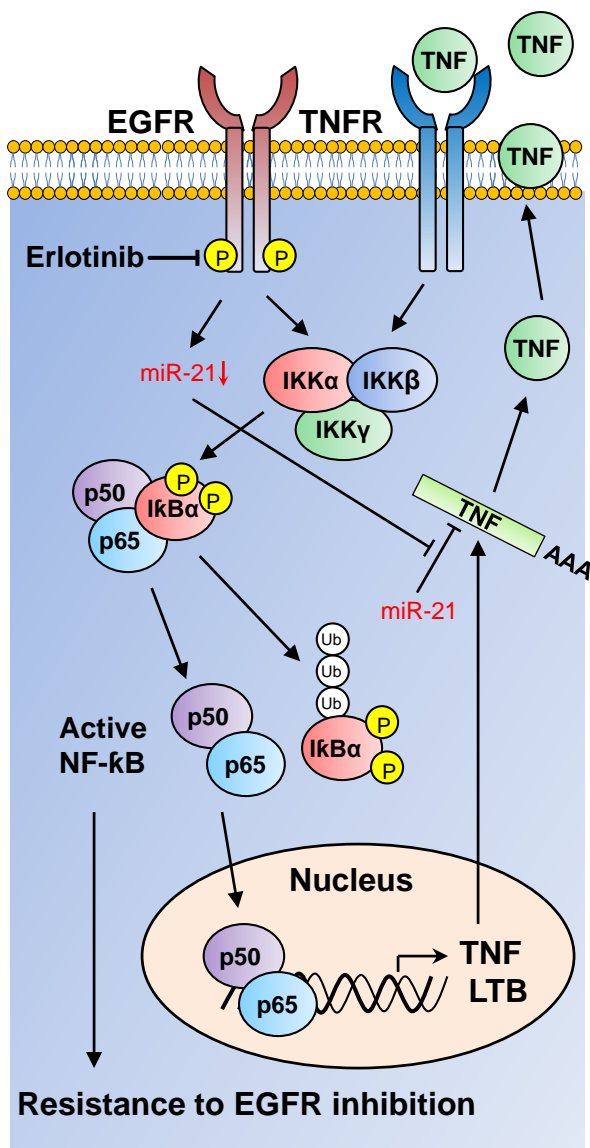


Sorafenib (N=50)

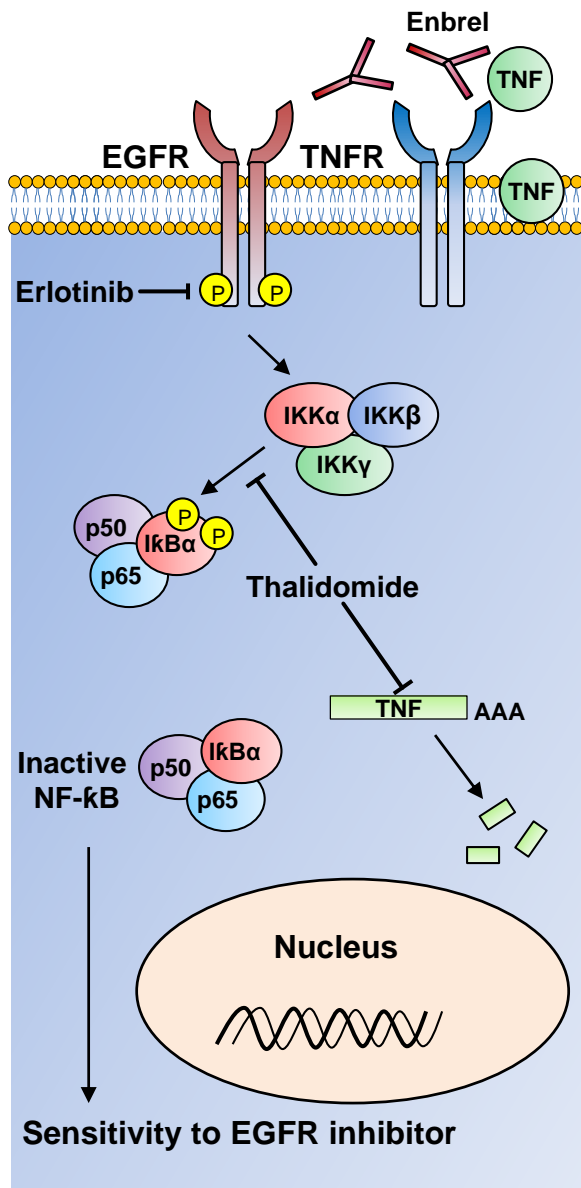
Supplementary Figure 20 TNF or NF- κ B target genes have no effect on outcomes of patients with Sorafenib treatment.

The clinical data of 50 patients assigned to Sorafenib therapy in the BATTLE trial and Progression-Free-Survival (PFS) were examined as described for erlotinib treated patients in Figure 10. TNF or NF- κ B target genes did not mitigate response to Sorafenib treatment. Low or high levels of gene were defined as lower or higher than the median value of 50 patients. The censored points were labeled with \perp .

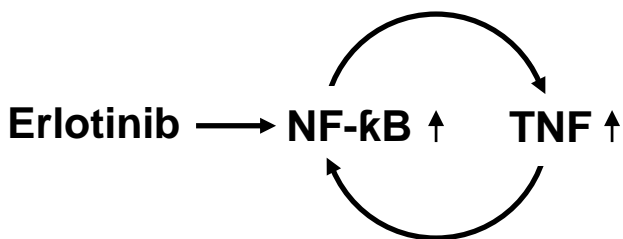
A



B



C



Supplementary Figure 21 Schematic of TNF signaling triggered by EGFR inhibition:

Depicting the adaptive response triggered by EGFR inhibition in our model. A. The left panel indicates that inhibition of EGFR leads to increased TNF mRNA via increased stability of TNF mRNA and increased NF- κ B mediated transcription of TNF. Increased TNF leads to NF- κ B activation in a feed-forward loop and also leads to upregulation of LT β which may mediate downstream effector function of TNF and NF- κ B. Activation of NF- κ B leads to resistance to EGFR inhibition induced cell death. B. The right panel shows that blocking the TNF-NF- κ B adaptive response renders lung cancer cells sensitive to EGFR inhibition. Etanercept (Enbrel) inhibits TNF signaling at the receptor level while thalidomide inhibits both NF- κ B activation and upregulation of TNF. C. Upon EGFR inhibition, NF- κ B activation and accumulation of TNF form a feedforward loop to enhance each other.

Supplementary Figure 22: Full length of western blots

Full-length Western blots for cropped images in main Figures and supplementary Fig. 7.

Supplementary Figure 23: Full length of western blots

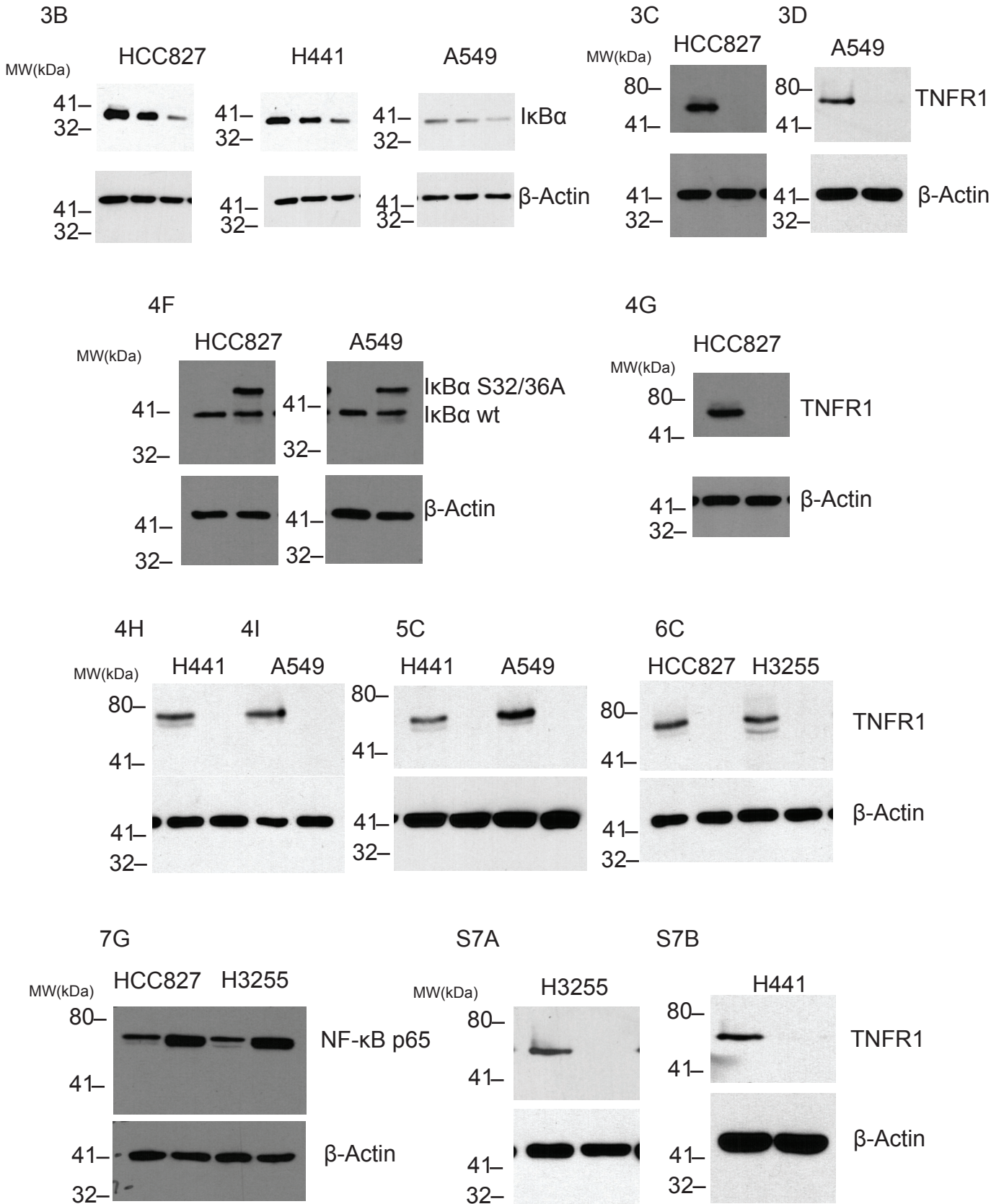
Full-length Western blots for cropped images in supplementary Fig. 9

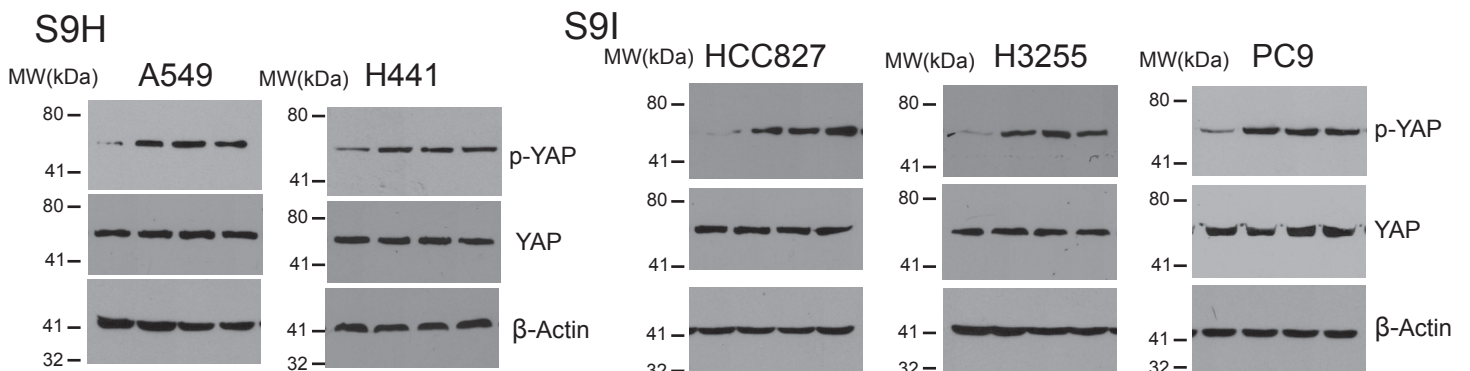
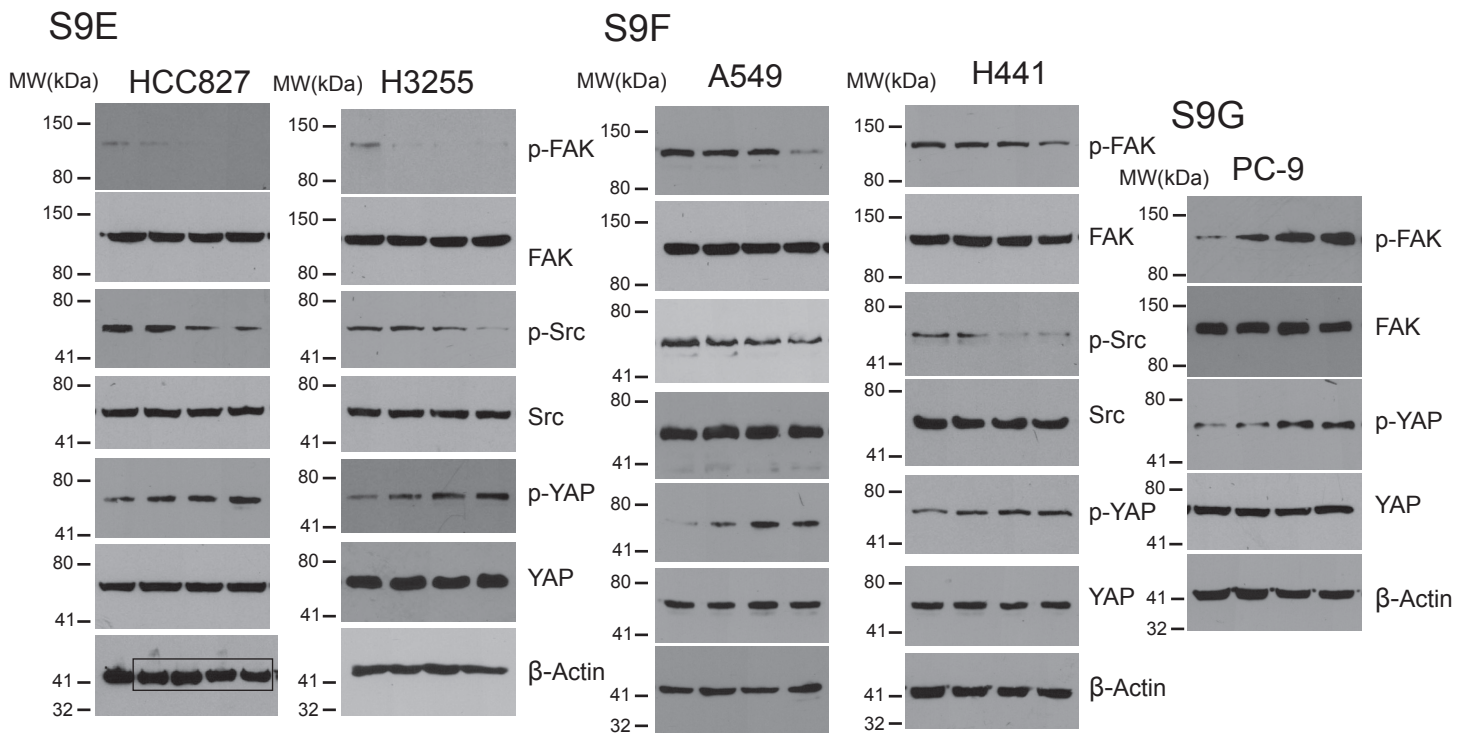
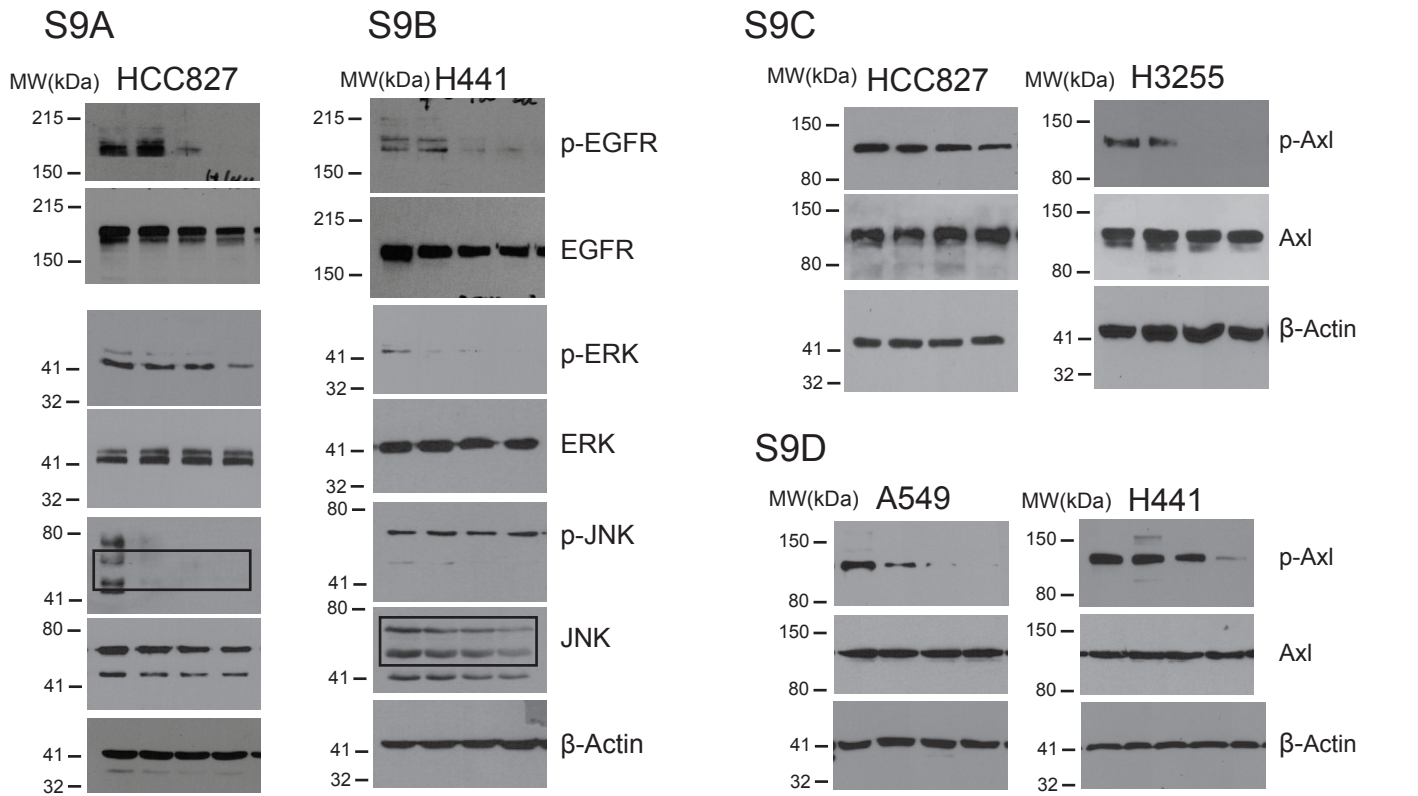
Supplementary Figure 24: Full length of western blots

Full-length Western blots for cropped images in supplementary Fig. 11, 14 and 17.

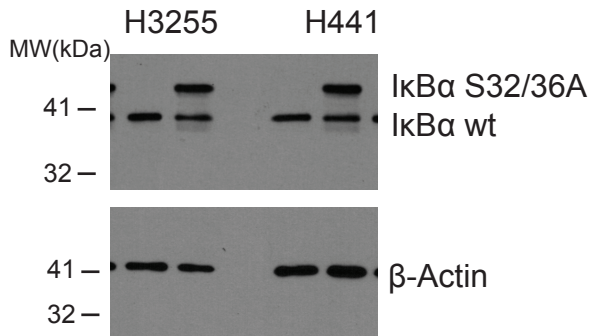
Supplementary Figure 22

Gong, Guo et al.

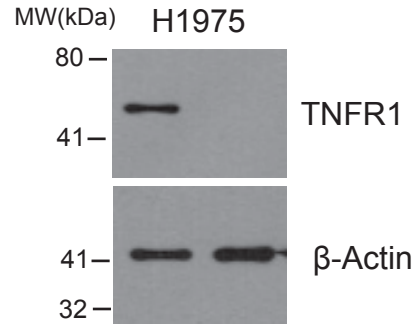




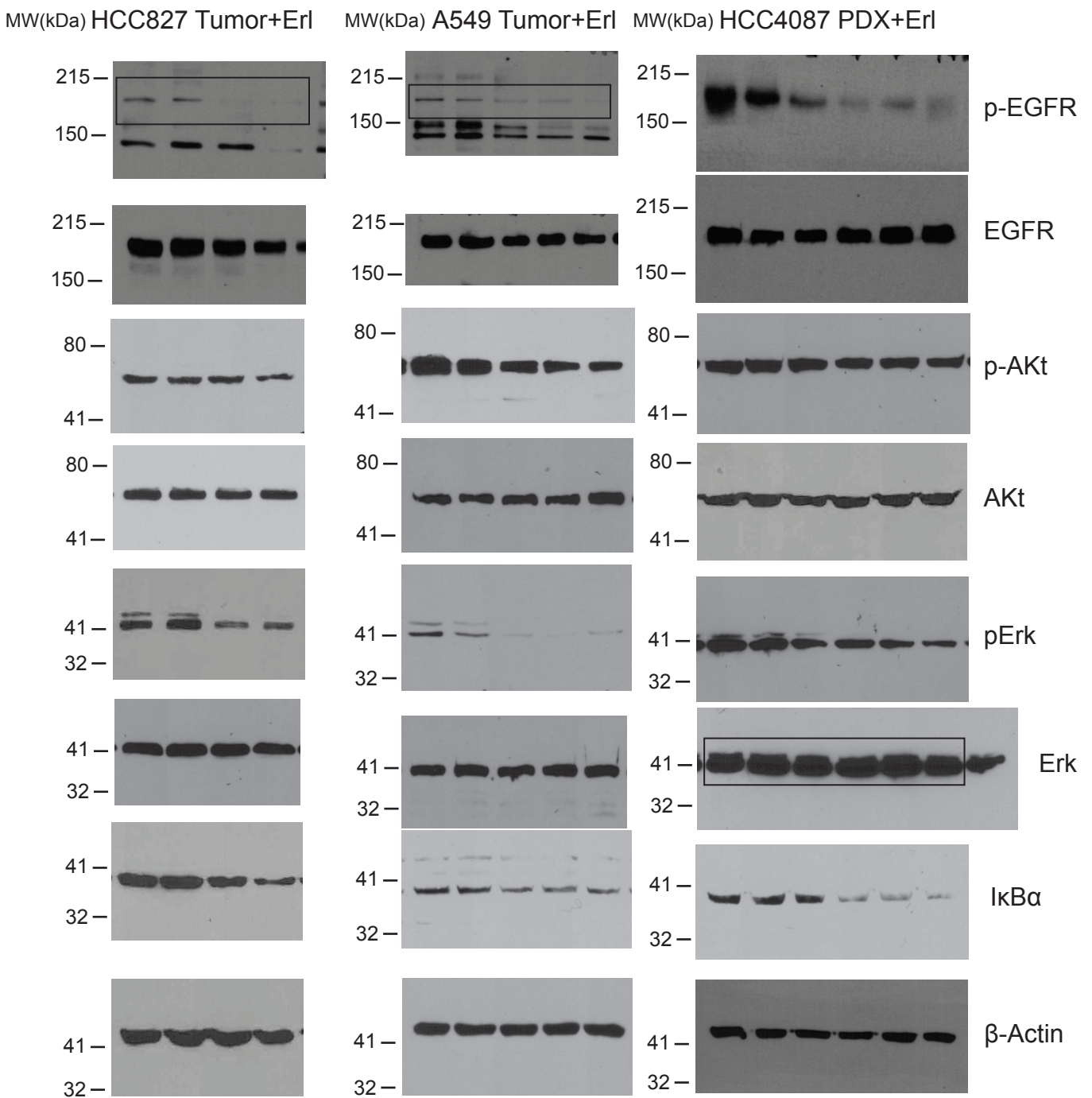
S11G



S14E



S17C



Supplementary Methods

Antibodies:

pEGFR(2236), pERK (4376), ERK (4695), pJNK (9251), JNK (9252), NF- κ B p65 (8242), I κ B α (4814), pFAK (8556), pSrc (2101), YAP (14074), pAkt (0915) antibodies were from Cell Signaling Technology (Danvers, MA); TNFR1 (sc-8436), FAK (sc-557), Src (sc-19), Akt (sc-1619), and β -Actin (sc-47778) were from Santa Cruz Biotechnology (Dallas, TX); EGFR (06-847) was from EMD Millipore (Billerica, MA); AXL antibody (AF154-SP) was from R&D (Minneapolis, MN); pYAP (ab62751) antibody was from Abcam (Cambridge, MA).

Luciferase assays

Cells were plated in 48 well dishes followed by transfection with NF- κ B-luciferase (LUC) plasmid or TNF 3'UTR luciferase reporter using lipofectamine 2000. A dual-luciferase reporter assay system was used according to the instructions of the manufacturer (Promega, Madison WI). Firefly luciferase activity was measured in a luminometer and normalized on the basis of Renilla luciferase activity. Experiments were done in triplicate and 3 independent experiments were done.

Chromatin Immunoprecipitation Assay

HCC827, H3255, H441, or A549 cells were plated in 15cm plates per reaction for ChIP assay (2×10^6 cells). The ChIP assay was carried out by using Chromatin Immunoprecipitation (ChIP) Assay Kit (Millipore) according to standard protocols (65). For qPCR 2 μ l of DNA from each reaction was mixed with SYBR Green Master Mix (Applied Biosystems, CA) and carried out in ViiA 7 Real-Time PCR System (Applied Biosystems). The data are expressed as percentage of input. Putative NF- κ B binding sites on TNF promoter were predicted by running AliBaba 2.1 program, and two sites were examined. The following 2 primer pairs were used: Region 1 (-

1909/-1636) covering putative NF- κ B binding site (-1812/-1801): 5'-CCGGAGCTTTCAAAGAAGGAATTCT-3' (forward) and 5'-CCCCTCTCTCCATCCTCCATAAA-3' (reverse); Region 2 (-1559/-1241) covering putative NF- κ B binding site (-1513/-1503): 5'-ACCAAGAGAGAAAGAAGTAGGCATG-3' (forward) and 5'-AGCAGTCTGGCGGCCTCACCTGG-3' (reverse).

MRI Imaging

MRI scans were conducted using a 7T small animal MRI scanner (Bruker, Rheinstetten, German) equipped with a 30 mm quadrature Radiofrequency (RF) coil. Under anesthesia by inhalation of 1.5 – 3% isoflurane mixed in with medical-grade oxygen *via* nose-cone, the animals were placed supine on a mouse holder, with a pneumatic respiratory sensor and Electrocardiography (ECG) electrodes for cardiac sensing, head first with the lung centered with respect to the center of the RF coil. The mice's chests were shaved and conducting hydrogels were applied to optimize ECG contact between electrodes and mouse. All MRI acquisitions were gated using both cardiac and respiratory triggering. The bore temperature was kept at 23 ± 2 °C to assure adequate and constant heart rate.

Two-dimensional (2D) scout images on three orthogonal planes (transverse, coronal and sagittal) were acquired to determine the positioning. Then, lower resolution gradient echo (GEMS) images were acquired on transverse plane in order to fine-adjust the slice position. Finally, higher resolution gradient echo images were recorded on the transverse plane, with the major parameters as follows: The repetition time (TR) = 200 ms (Note: the actual TR is changing according to ECG R-R interval, in range of 200 ms to 240 ms), the echo time (TE) = 1.966 ms, the flip angle (FA) = 45°, the number of average = 12, the field of view (FOV) = 32 x 32 mm², the matrix size = 256 x 256, the slice number = 17-21 (changed upon the mouse lung size), and the slice thickness = 1 mm without any gap.

Image analysis

The image analyses were performed using ImageJ, which is in public domain that developed by National Institutes of Health, the United States of America.

Virus infection

Adenovirus-GFP or I κ B α adenovirus were obtained from Vector Biolabs (Malvern, PA). An Multiplicity of infection (MOI) of 10 was used in the experiments. Cells were exposed to adenovirus in the presence or absence of Erlotinib for 72h followed by Cell viability assay or Western blotting.

Human shTNF Lentiviral Particles and Control shRNA Lentiviral Particles-A were purchased from Santa Cruz Biotechnology (Dallas, TX). Cells were infected with shRNA lentiviral particles following the manufacturer's protocol and 0.6 μ g/mL puromycin was added for selecting stable clones.

Establishment of PDX model:

The NSCLC specimen (P0) was surgically resected from a patient diagnosed with adenocarcinoma/squamous cell carcinoma, IIB, T3, at UT Southwestern, after obtaining Institutional Review Board approval and informed consent. It has KRAS G13C mutation but no EGFR activating mutations in the normal lung or lung tumor detected by Exome sequencing. 4 to 6 weeks old female NOD SCID mice were purchased from Charles River Laboratories. The PDX tumor tissues were cut into small pieces (~20 mm³) and subcutaneously implanted in NOD SCID mice of serial generations (P1, P2, etc.). P4 tumor bearing SCID mice were used in this study.

Immunohistochemistry and TUNEL staining

Experiments were performed on tumor xenografts from mice fixed in 10% formalin and embedded in paraffin or on human lung cancer paraffin sections. Immunohistochemical staining was performed using the ABC streptavidin–biotin method with the Vectastain ABC kit (Vector Laboratories, Burlingame, CA, USA) according to the manufacturer's protocol. Briefly, sections were deparaffinized and dehydrated, endogenous peroxidase activity was quenched by a 10 min incubation in 3% H₂O₂. For antigen retrieval, the tissue sections were boiled in 10 mM sodium citrate buffer (pH 6.0) for 20 minutes. Samples were then incubated overnight with an anti-Nuclear localization signal (NLS) p65 (1:100, Cell Signaling Technology, 4376,) or anti-Ki76 antibody (1:200, Cell signaling Technology, 4668) at 4°C. The signal was detected by using the Sigmafast 3,3'-Diaminobenzidine tablets (DAB; Sigma, St. Louis MO). The sections were counterstained lightly with hematoxylin. Three to four complete and non-overlapping high magnification (x400) fields were randomly selected for each section. For Ki-67 and NLS p65, the percentage of positively stained nuclei out of the total cells counted was evaluated. TUNEL staining was performed using the TUNEL assay kit (4810-30-K, R&D Systems, Minneapolis, Minnesota, USA) according to the manufacturer's instructions.

PCR array

A549 cells were treated with 1 μM Erlotinib or Dimethyl sulfoxide (DMSO) for 24 hours. The extracted RNA was subjected to Human NF-κB Signaling Targets PCR Array (Qiagen, PAHS-225Z) on a ViiA 7 Real-Time PCR System (Thermo Fisher Scientific) according to the manufacturer's instructions.

Colony formation assay

Cells were seeded in 6 well plates at 1000 cells/well, and incubated with indicated drugs. 7 days later, cell colonies were fixed by 100% methanol and then stained by 0.5% crystal violet in 25%

methanol. Images were captured by a scanner and colony counts were processed by ImageJ. Three independent experiments were done.

MicroRNA studies:

For microRNA inhibition, we obtained miRNA inhibitors from IDT (Coralville, IA). The mature sequence of hsa-miR-21-5p was achieved from www.mirbase.org as uagcuuaucagacugauguuga; The human negative control miRNA inhibitor sequence was proposed by IDT as ucguuaaucggcuauaauacgc. For miRNA overexpression, miR-21 mimics and negative control mimic were ordered from Qiagen (Germantown, MD): Syn-hsa-miR-21-5p: 5'UAGCUUAUCAGACUGAUGUUGA. miRNA inhibitors and mimics were transfected into cultured cells by a method similar to siRNA transfection, using Lipofectamine 2000 reagent.

ELISA

To detect TNF levels in medium, cells were cultured in serum free medium and treated with indicated drugs for 48 hours. Supernatant was then collected and concentrated using a Pierce protein concentrator (Thermo-Fisher). To test TNF in lysates, cell and tumor lysates were extracted following standard protocols used for Western blot. Total protein concentrations were determined by Pierce BCA Protein Assay Kit (Fisher Scientific). Then, the levels of TNF protein were measured by ELISA using a commercial TNF detection kit (Fisher Scientific) according to the manufacturer's protocol. LTB (TNFC) expression levels in cells were tested by TNFC Colorimetric Cell-Based ELISA Kit (OKAG01301) (Aviva Systems Biology, San Diego, CA). Cells were seeded in 96-well plates and treated with indicated drugs for 24 hours. ELISA was performed according to the manufacturer's protocol. GAPDH antibody supplied in the kit was used as the loading control.

Real Time PCR

Each PCR reaction was carried out in triplicate in a 20 μ L volume using SYBR Green Master Mix (Applied Biosystems) for 15 minutes at 95°C for initial denaturing, followed by 40 cycles of 95°C for 15 s and 60°C for 60s in ViiA 7 Real-Time PCR System (Applied Biosystems). At least three independent experiments were done. Values for each gene were normalized to expression levels of GAPDH mRNA. Primer sequences were as below. TNF: 5'-CCCAGGGACCTCTCTAATCA-3' (forward) and 5'-GCTACAGGCTTGTCCTCGG-3' (reverse); GAPDH: 5'-GTGAAGGTCGGAGTCAACGG-3' (forward) and 5'-TGATGACAAGCTTCCCGTTCTC-3' (reverse). LTB and IL2RA primers were purchased from MilliporeSigma (St. Louis, MO), H_LTB_1 and H_IL2RA_1.

Supplementary Table 1

Gong, Guo et al.

Gene	A549	Calu-3	H1373	H1573	H1650	H1666	H1975	H2122	H322	H3255	H441	H820	HCC2279	HCC2935	HCC4006	HCC4011	HCC827	PC-9
EGFR†	WT	WT	WT	WT	Mutant	WT	Mutant	WT	WT	Mutant	WT	Mutant	Mutant	Mutant	Mutant	Mutant	Mutant	Mutant
KRAS†	Mutant	WT	Mutant	Mutant	WT	WT	WT	Mutant	WT	WT	Mutant	WT	WT	WT	WT	WT	WT	WT
FGFR1†	WT	WT	WT	WT	WT	Mutant	WT	WT		WT			WT		WT			WT
RICTOR†	WT	WT	WT	WT	WT	WT	WT	WT		WT			WT		WT			WT
PTEN†	WT	WT	WT	WT	Mutant	WT	WT	WT		WT			WT		WT			WT
ALK†	WT	WT	WT	WT	WT	WT	WT	WT	Mutant	WT			WT		WT			WT
DDR2†	WT	WT	WT	WT	WT	WT	WT	WT		WT	Mutant		WT		WT			WT
ERBB2†	WT	WT	WT	WT	WT	WT	WT	WT	Mutant	WT	WT	WT	WT	WT	WT	WT	WT	WT
MET†	WT	WT	WT	WT	WT	WT	WT	WT		WT			WT		WT			WT
NTRK1†	WT	WT	Mutant	WT	WT	WT	WT	WT		WT			WT		WT			WT
BRAF†	WT	WT	WT	WT	WT	Mutant	WT	WT	WT	WT	WT	WT	WT	WT	WT	WT	WT	WT
PIK3CA†	WT	WT	WT	WT	WT	WT	Mutant	WT	WT	WT	WT	WT	WT	WT	WT	WT	WT	WT
ROS1†	WT	WT	WT	WT	WT	WT	WT	WT		WT			WT		WT			WT
FGFR3†	WT	WT	WT	WT	WT	WT	WT	WT		WT			WT		WT			WT
AKT1†	WT	WT	WT	WT	WT	WT	WT	WT		WT			WT		WT			WT
MAP2K1†	WT	WT	WT	WT	WT	WT	WT	WT		WT			WT		WT			WT
NRAS†	WT	WT	WT	WT	WT	WT	WT	WT		WT			WT		WT			WT
RET†	WT	WT	WT	WT	WT	Mutant	WT	WT		WT		Mutant	WT		WT			WT
TP53	WT	Mutant	Mutant	Mutant	Mutant	WT	Mutant	Mutant	Mutant	Mutant	Mutant	Mutant	Mutant	Mutant	Mutant	Mutant	Mutant	Mutant
CDKN1A	WT	Mutant	WT	WT	WT	WT	WT	WT		WT			WT		WT			WT
NFKB1	WT	WT	WT	WT	WT	WT	WT	WT		WT			WT		WT			WT
NFKB2	WT	WT	WT	WT	WT	WT	WT	WT		WT		Mutant	WT		WT			WT
RELA	WT	WT	WT	WT	WT	WT	WT	WT		WT			WT		WT			WT
RELB	WT	WT	WT	WT	WT	WT	WT	WT		WT			WT		WT			WT
REL	WT	WT	WT	WT	WT	WT	WT	WT		WT			WT		WT			WT
IKBKB	WT	WT	WT	WT	WT	WT	WT	WT		WT			WT		WT			WT
IKBKG	WT	WT	WT	WT	WT	WT	WT	WT		WT			WT		WT			WT
NFKBIA	WT	WT	WT	WT	WT	WT	WT	WT		WT			WT		WT			WT
TNF	WT	WT	WT	WT	WT	WT	WT	WT		WT			WT		WT			WT
TNFRSF1A	WT	WT	WT	WT	WT	WT	WT	WT		WT			WT		WT			WT
TNFRSF1B	WT	WT	WT	WT	WT	WT	WT	WT		WT			WT		WT			WT
IL2RA	WT	WT	WT	WT	WT	WT	WT	WT		WT			WT		WT			WT
LTB	WT	WT	WT	WT	WT	WT	WT	WT		WT			WT		WT			WT
PDGFB	WT	WT	WT	WT	WT	WT	WT	WT		WT			WT		WT			WT
IL12B	WT	WT	WT	WT	WT	WT	WT	WT		WT			WT		WT			WT
CCL22	WT	WT	WT	WT	WT	WT	WT	WT		WT			WT		WT			WT
TRAF2	WT	WT	WT	WT	WT	WT	WT	WT		WT			WT		WT			WT

Supplementary Table 1: Oncogenes and TNF/NFKB-associated genes mutant status in NSCLC lines used in this study

†**Mutant oncogenes in lung cancer:** Lovly, C., L. Horn, W. Pao. 2016. Molecular Profiling of Lung Cancer. My Cancer Genome <https://www.mycancergenome.org/content/disease/lung-cancer> (Updated March 28, 2016).

Data Sources: 1. COSMIC (Catalogue Of Somatic Mutations In Cancer)-v76 <http://cancer.sanger.ac.uk/cosmic> (Updated February 16, 2016); 2. Data from a CPRIT (Cancer Prevention & Research Institute of Texas)-funded NGS (next generation sequencing) project by Dr. John Minna, UT Southwestern Medical Center. Data from Dr. Adi Gazdar, UT Southwestern Medical Center.

WT: No mutation was found in any of those 3 data sources.

Mutant: There is at least one mutation reported from those 3 data sources.

Blank: It was not tested in all 3 data sources.